Jayakumari, S., V. Canaguier, H. Dalaker, C. Van der Eijk, and M. Ksiazek. 2026. Developing Optimized Agglomerates for Silicon and Ferroalloys industries. In *Silicon for the Chemical and Solar Industry XVIII*, edited by M. Tangstad, H. Rong, A. Valderhaug, B. Andresen, H. Dalaker, and I. G. Page. Kristiansand, Norway, September 7–10. https://doi.org/10.55669/oa900823

Developing Optimized Agglomerates for Silicon and Ferroalloys industries

Sethulakshmy Jayakumari[1], Vincent Canaguier[1], Halvor Dalaker[1], Casper Van der Eijk[1] and Michal Ksiazek[1]

[1]SINTEF, Norway, Sethulakshmy.Jayakumari@sintef.no

Keywords: Bio-carbon agglomerates, Pellets, Briquettes, SiO-reactivity, CO_2-reactivity, Strength

Abstract – The ferroalloy industry aims to reduce CO_2 emissions and achieve carbon-neutral production by 2050 by replacing fossil carbon with renewable biocarbon and developing sustainable process technologies. Although charcoal is already used as a reductant in ferroalloy production, its lower mechanical strength and higher fines generation compared with fossil carbon materials limit its use in large, closed furnaces, particularly in Norway. Therefore, improved biocarbon materials are needed to enable wider industrial adoption. This study focuses on developing sustainable, high-performance biocarbon agglomerates derived from biomass and waste/byproducts for silicon and ferroalloy production. It also focuses on improving the mechanical durability of renewable reductants through agglomeration techniques such as extrusion and briquetting, enabling the production of biomass pellets and briquettes. Strength enhancement is essential to minimize fines formation during transportation, storage, and furnace operation, thereby ensuring predictable carbon availability and stable carbon balance in industrial processes.

The study systematically investigates key agglomeration parameters - including particle size distribution, binder selection, and applied compaction pressure - and their influence on pellet strength, porosity, and gas reactivity. Laboratory-scale testing evaluated the durability and gas reactivity of the developed agglomerates to identify optimal processing conditions. Overall, the results demonstrated that charcoal fines can be successfully agglomerated into mechanically robust and thermally stable materials with properties suitable for ferroalloy production processes. The outcomes supported the transition toward carbon neutral ferroalloy production by providing mechanically robust, reactive, and sustainable biocarbon-based reductants suitable for industrial furnace applications.

Graphical abstract

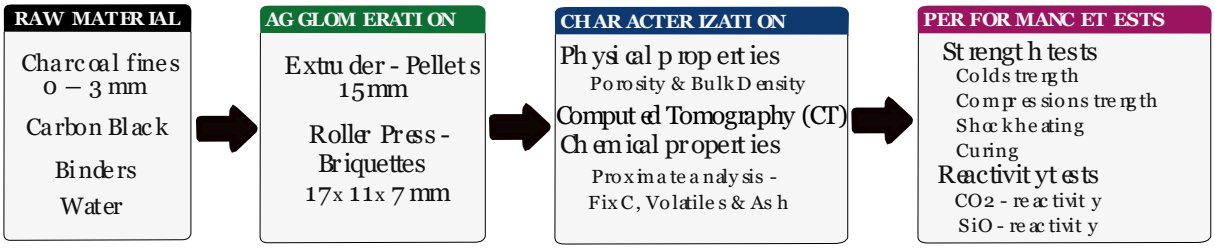

1. INTRODUCTION

Ferroalloys and silicon production play a vital role in modern industry and technologies, particularly in steel making, renewable energy systems and advanced electronic applications. These processes largely depend on carbonaceous reductants, to perform the carbothermic reduction of metal oxides in high temperature furnaces, traditionally using fossil based materials such as coal, coke and petroleum coke while also incorporating charcoal as part of the reductant mix in some operations. (Schei, Tuset and Tveit, 1998; Olsen, Tangstad and Lindstad, 2026). This significantly affects greenhouse gas emissions from metallurgical industries, thereby contributing to climate change (Lindstad et al., 2007a; Tangstad and Ringdalen, 2025). In response to the increasing environmental concerns and strict climate policies, there is a strong global commitment to achieve carbon neutrality by 2050. According

to Prosess21 report "New Process Technology for Reduced Carbon Footprint, including CCU", industrial greenhouse gas emissions especially in Norway are to be phased out by 2050 (Prosess21 ekspertgrupperapport, 2021). To achieve these ambitious targets, increased research and development of carbon neutral processes is essential. Although Norway already uses renewable hydropower making its production cleaner compared to many other countries, fossil carbon is still used in the furnaces, resulting in significant CO_2 emissions during metal production. The CO_2 footprint from the silicon and ferroalloy production is directly linked to the consumption of fossil reductants, with emissions of several tonnes of CO_2 per tonne of metal produced. Typical emissions range from 1.4 to 6.9 t CO_2 per tonne of ferroalloy and 2.5 to 4.8 t CO_2 per tonne of for ferrosilicon (FeSi) (Han and Tangstad, 2024). A promising solution is to replace fossil-based reductants with renewable carbon sources, in particularly with biocarbon derived from biomass. In response to these challenges, the ferroalloy industries aim to replace fossil carbon with biocarbon, targeting a 40–50% reduction in CO_2 emissions by 2030, and further progressing towards fully carbon neutral processes by 2050. (Sommerfeld and Friedrich, 2021; Han and Tangstad, 2024; Hoover, Bell and Rippy, 2024)

Biocarbon is a renewable and CO_2 neutral source of carbon, since the CO_2 released during its use is balanced by the CO_2 absorbed during the growth of biomass. Because of this, the use of biomass-based materials in metallurgical process has received increasing research attention. But despite known benefits, the industrial use of biocarbon is still limited due to its weaker physical and mechanical properties compared to conventional coal and coke. (Smith-Hanssen, Jahrsengene and Ringdalen, 2023a; Han and Tangstad, 2024). Some of the main limitations of biocarbon, particularly charcoal, are its low mechanical strength, high porosity, and poor structural integrity. These properties lead to significant degradation during handling, transportation, and furnace operation, resulting in the generation of fines. In industrial silicon production, it has been reported that more than 10% of charcoal can be lost as fines due to abrasion (Jayakumari and Ksiazek, 2024). The presence of these fines in submerged arc furnaces negatively affects burden permeability, gas flow distribution, and process stability, ultimately reducing furnace efficiency and operational reliability (Makgobelele et al., 2021; Han and Tangstad, 2024; Jayakumari and Ksiazek, 2024).

To address these challenges, agglomeration techniques such as extrusion, briquetting, and pelletizing have been proposed as effective solutions to improve the handling and performance of biocarbon materials. These techniques convert fine materials into compact, high-density agglomerates with uniform size and shape, enhancing their mechanical durability and suitability for industrial applications (Karunanithy et al., 2012).

Many ferroalloy and silicon plants possess significant quantities of underutilized carbon resources in the form of charcoal fines that cannot be directly add into the furnaces. With the growing demand for biocarbon in metallurgical applications, it becomes increasingly important to utilize all available biomass resources efficiently. In addition to the conventional lump charcoal, significant quantities of carbon rich residues are generated throughout the biomass value chain, including fines from pyrolysis process, sawdust from wood processing industries etc. The conversion of such residual biomass into useful products is a key element of circular bioeconomy strategies, where waste streams are valorised into high-value materials, reducing environmental impact and improving resource efficiency (Obi, Pecenka and Clifford, 2022; Olofsson, 2025). Although agglomeration through briquetting or pelletizing appears to be an intuitive solution to recover these materials, practical implementation often faces critical challenges. A common limitation in existing approaches is the emphasis on cold mechanical strength, which primarily addresses handling, storage, and transportation requirements. However, the performance of agglomerates under actual furnace conditions is governed by their thermal stability, or hot strength, so binder selection is crucial. In submerged arc furnace (SAF) operation, agglomerates are exposed to rapid temperature gradients and mechanical stresses within the reaction zone. If the binder system and curing conditions are

not properly optimized, agglomerates may undergo degradation due to thermal shock. This can result in the formation of fines within the furnace; Therefore, the design of biocarbon agglomerates must extend beyond cold strength considerations to ensure adequate performance under high-temperature process conditions.

Optimizing agglomerated biocarbon requires careful control on both mechanical and chemical properties. While increasing compaction pressure, binder content and addition of water can significantly affect strength and durability. Furthermore, different metallurgical processes impose distinct requirements on the properties of carbon reductants. Some processes require materials with high porosity and sufficient mechanical strength to ensure gas reactivity and permeability, on the other hand other processes may benefit from denser materials with low reactivity to achieve controlled and stable reduction behaviour (Kaffash, Surup and Tangstad, 2021). This highlights the need for process specific design of agglomerates, where the balance between mechanical strength, porosity, and reactivity must be carefully optimised (Jayakumari and Ksiazek, 2024).

Several key parameters govern the performance of agglomerated biocarbon, including particle size distribution, binder type and amount, moisture content, applied compaction pressure and curing conditions. These parameters significantly influence the internal structure, density, porosity, and gas reactivity of the final agglomerated product. Mechanical strength, thermal behaviour and performance under high temperature conditions are also affected (Olugbade, Ojo and Mohammed, 2019; Zhang et al., 2020). Although previous studies have investigated individual aspects of biomass densification, there remains a lack of systematic and application-specific research focused on optimizing agglomerates for silicon and ferroalloy production (Karunanithy et al., 2012).

The present study aims to develop sustainable and high-performance biocarbon agglomerates derived mainly from charcoal fines as well as carbon black. The work focuses on optimizing agglomeration techniques such as extrusion and briquetting to produce agglomerated pellets and briquettes with mechanical durability and controlled reactivity at high temperature conditions. Laboratory scale investigations are conducted to evaluate both the physical and chemical properties, mechanical strength, and gas reactivities and compare their performances with that of charcoal, coal and metallurgical coke, the latter being the coke (made form coking coal) typically used in the manganese ferroalloy production. The outcomes of this research are expected to provide valuable insights into the design of robust and sustainable carbon materials with optimal reactivity, thereby supporting the transition towards carbon neutral silicon and ferroalloy production.

2. MATERIALS AND METHODS

2.1 Materials

Charcoal fines (CC-17) in the particle range of 0–3 mm were used as the primary carbon source in this study. These materials were supplied by **OZEN Sp. Z o.o.**, a leading producer of certified charcoal. Regarding carbon black, the sources are anonymized for confidentiality reasons. To produce charcoal-based agglomerates, a range of binders was utilized including Ca-, Na- and NH_3- based lignosulphonates, wheat starch and solid pyrolytic lignin (SPL) (Narron, Wolken and Gargulak, 2020; Butler, Skrivan and Lotfi, 2023). These binders were provided by established industrial suppliers, namely **Borregard**, **Crespel & Deiters** and **BTG group**. In addition, commercially available bentonite was included in some of the binder mix. Microsilica, sourced from an industrial silicon production plant was also investigated as a potential binding agent in the production of extruded pellets to examine its influence on strength and high temperature behaviour. Furthermore, quartz-charcoal composite pellets were produced separately via extrusion to examine the feasibility of manufacturing such

composite materials using this technique. The carbon black pellets were produced using two carbon black types and bio binders. Due to confidentiality, the specific details regarding the composition and formulation of the binders cannot be disclosed. It should be noted that these pellets were not produced as part of present study, but these were developed as a part of the MECALO project by **ITPE** (Institute of Energy and Fuels Processing Technology, Zabrze, Poland).

The carbon source, binding agents and the produced pellets and briquettes are shown in figure 1. Table 1 presents the abbreviations used for the carbon and binder materials in the different pellet and briquette recipes. Charcoal (CC-16), coal (C-17) and coke (CK-009), acquired from ferroalloys industries, were used as reference materials.

Figure 1: Raw materials used for producing charcoal pellets and briquettes

Table I. Abbreviations used for carbon and binder materials

Charcoal - **CC**	Starch - **S**
Coal - **CL**	Solid Pyrolytic Lignin - **SPL**
Coke - **CK**	Bentonite - **B**
Carbon Black - **CB**	Quartz - **Qz**
Pellets - **PLT**	Microsilica - **M**
Briquettes - **BRQT**	**Ca, Na, NH_3** – Calcium-, Sodium-, Ammonium-Lignosulphonates

2.2 Extrusion and Briquetting

Prior to extrusion, all raw materials were thoroughly premixed using a laboratory mixer to ensure homogeneous distribution of biomass, binders, and moisture.

Extrusion of charcoal pellets was carried out using a laboratory-scale extruder (DEX Lab, Verdes). The extruder consists of an inlet hopper, a pre-compression unit equipped with

mixing knives, a vacuum chamber, and an extrusion body. The premixed material was fed through the hopper into the pre-compression unit, where it was further conditioned to facilitate smooth transport by the augers. The material was then conveyed into the next chamber and subsequently extruded into pellets.

A die size of 15 mm was used for all extrusion experiments to produce uniform pellets. The operating conditions were adjusted by varying the auger speed within a frequency range of 20–30 Hz. The extrusion parameters were optimized depending on material characteristics such as particle size, binder type, and moisture content to ensure stable pellet formation. A schematic illustration of the extrusion set up, including the pre-mixer, extruder and extrusion die is shown in figure 2 while the schematic illustration of the briquetting machine is shown in figure 3.

Charcoal fines briquettes were produced using a laboratory-scale roller press (B050), with a processing capacity of 1–45 kg/h depending on material properties and operating conditions. Prior to briquetting, the raw materials including charcoal fines, binders, and water were thoroughly premixed in a separate mixer to ensure homogeneity. The prepared mixture was fed into the briquetting machine through the feed hopper, from where it was transported via vertical and horizontal screw feeders into the nip zone. Briquetting was achieved by compressing the material between two counter-rotating rolls under applied hydraulic pressure. The operating parameters, including screw and roll speeds, were adjusted using variable speed drives to ensure stable briquette formation. The briquettes produced had approximate dimensions of 17×11×7 mm, using rolls with a diameter of 100 mm and a width of 20 mm.

It should be noted that carbon black (CB) pellets were not produced using the same methodology as in the present study, and detailed information regarding their production process is not disclosed.

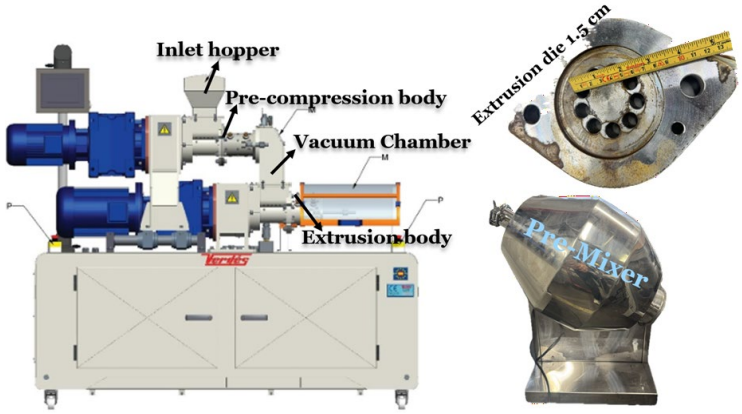

Figure 2. Schematic illustration of the extrusion set up, including the pre-mixer, extruder and extrusion die.

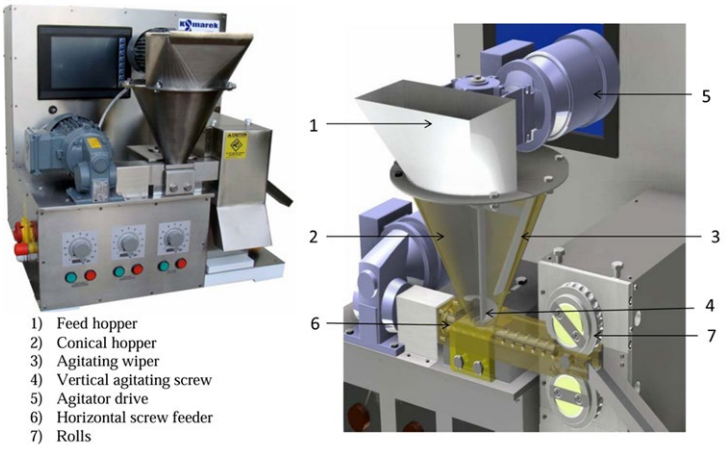

Figure 3. Schematic illustration of the briquetting machine

A stage-gate approach was used to evaluate carbon materials for Mn and Si processes (Smith-Hanssen, Jahrsengene and Ringdalen, 2023a). Mechanical properties were assessed first to exclude unsuitable materials, followed by reactivity testing for the selected materials. Materials were characterised under process relevant conditions using experimental procedures developed at SINTEF and NTNU. This approach enables systematic evaluation of carbon materials considering their multiple roles in metallurgical process.

Porosity was determined by combining skeletal and envelope density measurements using an AccuPyc gas pycnometer using helium gas displacement and a GeoPyc displacement pycnometer respectively.
Figure 4 shows the porosity measured for one briquette (BRQT), five different charcoal pellets (PLT) produced using different binder compositions, three selected silicon carbide (SiC) pellets after the SiO reactivity test, two carbon black (CB) pellets, two types of charcoal (CC), one coal (CL) and one coke (CK-009). Interestingly, the porosity of all pellets, the briquette and the SiC converted pellet samples fall within the value observed for coal. However, the conventional carbon materials show a clear difference in porosity, with charcoal exhibiting the highest porosity followed by coal and then coke.

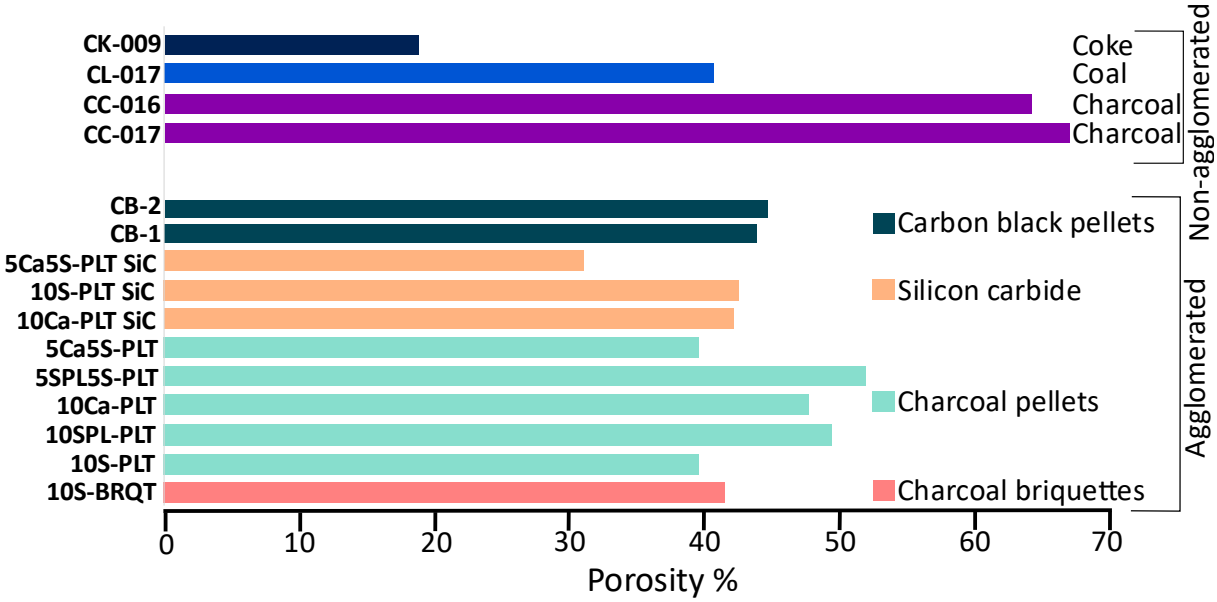

Figure 4. Porosity values for the agglomerated charcoal materials, carbon pellet converted SiC samples (after the SiO reactivity test), carbon black pellet sand the conventional carbon materials.

Bulk density was measured by filling a 100 mL beaker with the sample and determining its mass. The bulk density was then calculated as the ratio of sample mass to the known volume of the beaker. Figure 5 presents the measured bulk densities of the pellets, briquettes and conventional carbon materials. The agglomerated pellets and briquettes exhibit relatively higher bulk densities in the range of 0.30–0.40 g/cm^3, which is comparable to that of coal. Among the agglomerated samples, the carbon black pellet (CB-2) shows the highest bulk density, exceedingly even that of coke. In contrast, both charcoal samples display lower bulk densities, with noticeable variation in both.

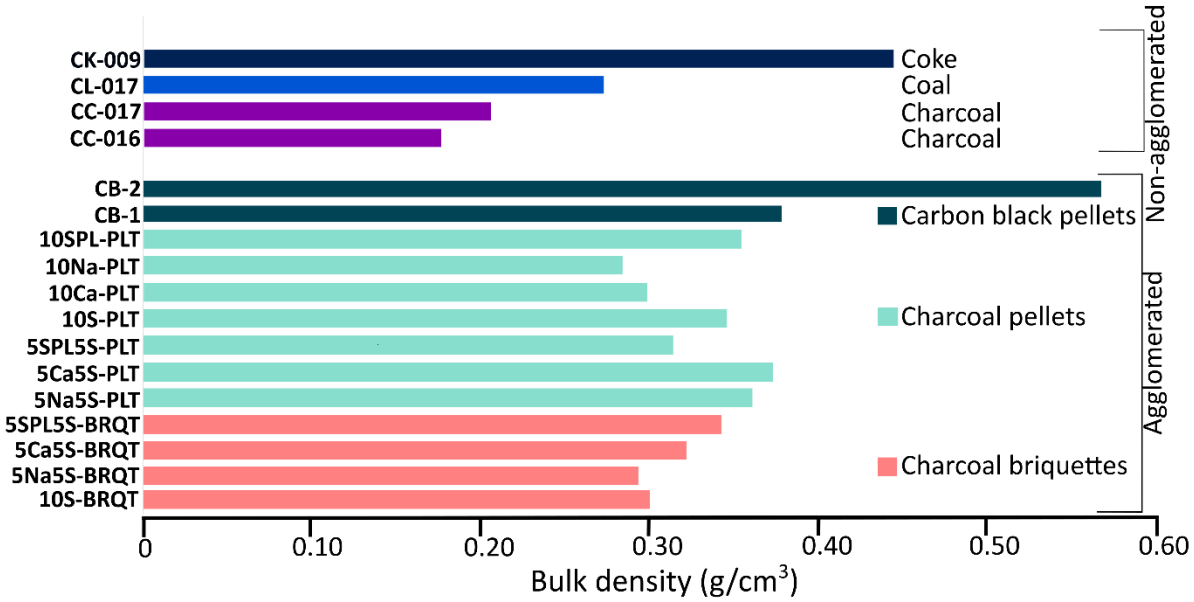

Figure 5. The measured bulk densities of the pellets, briquettes and conventional carbon materials.

Bulk density and porosity show an inverse relationship, where higher porosity generally results in lower bulk density (Jayakumari and Ringdalen, 2022). The agglomerated pellets and briquettes exhibit moderate porosity and relatively higher bulk densities similar to coal. In contrast charcoal samples display higher porosity which corresponds to their lower bulk densities. The carbon black pellet (CB-1) shows higher bulk density indicating a more compact structure with reduced pore volume. Overall, these trends confirm that variations in porosity strongly influence the bulk density of the materials.

A micro-X-ray computed tomography (µCT) analysis was conducted to evaluate the internal structure of the pellets such as the distribution and incorporation of the binder and the particle size distribution within the pellets. Figure 6 presents CT-images of charcoal and coal, figure 7 shows different agglomerated pellets and figure 8 shows pellets produced using charcoal-microsilica and charcoal-quartz mixtures. The pores in charcoal are relatively large and uniformly distributed, whereas coal exhibits a more heterogeneous pore structure with regions of both large pores and dense areas. In the agglomerated pellets, both pores and particles of varying sizes are more homogeneously distributed, resulting a dense structure. A clear influence of the binder on pellets structure is observed. The use of SPL as a binder made pellet production more challenging, leading to the development of cracks in the final pellets. Additionally, pellets containing microsilica and quartz demonstrate that such composite materials can be successfully produced using extrusion process.

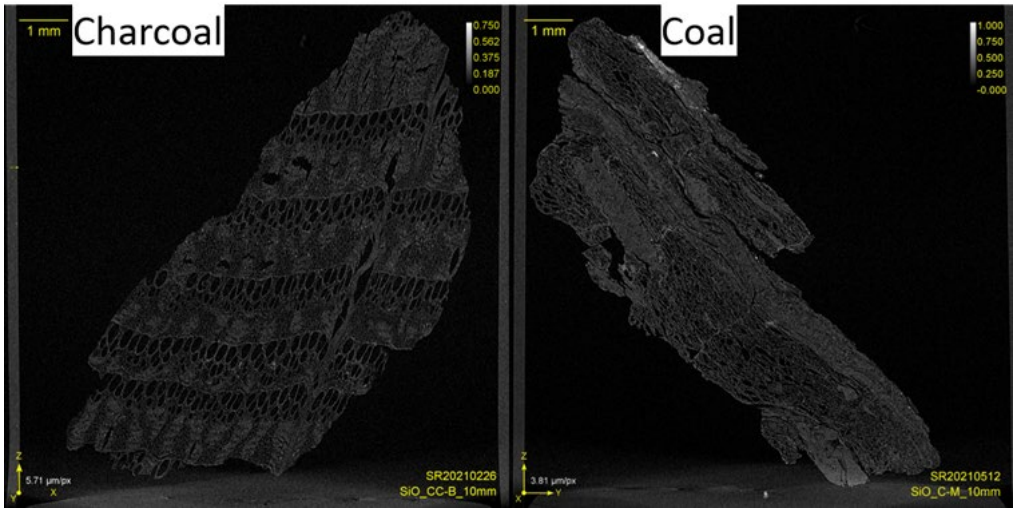

Figure 6. CT-images of charcoal and coal

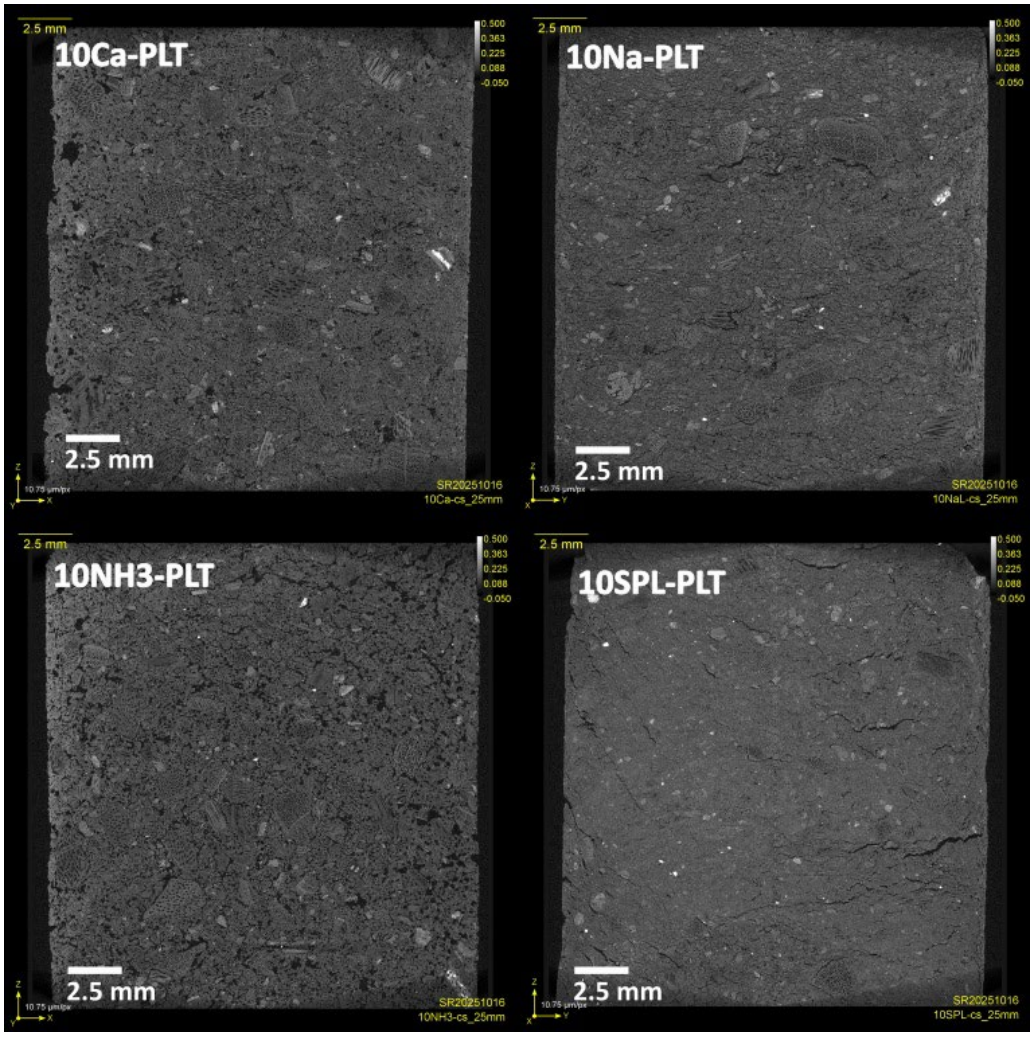

Figure 7. Extruded pellets with different binders

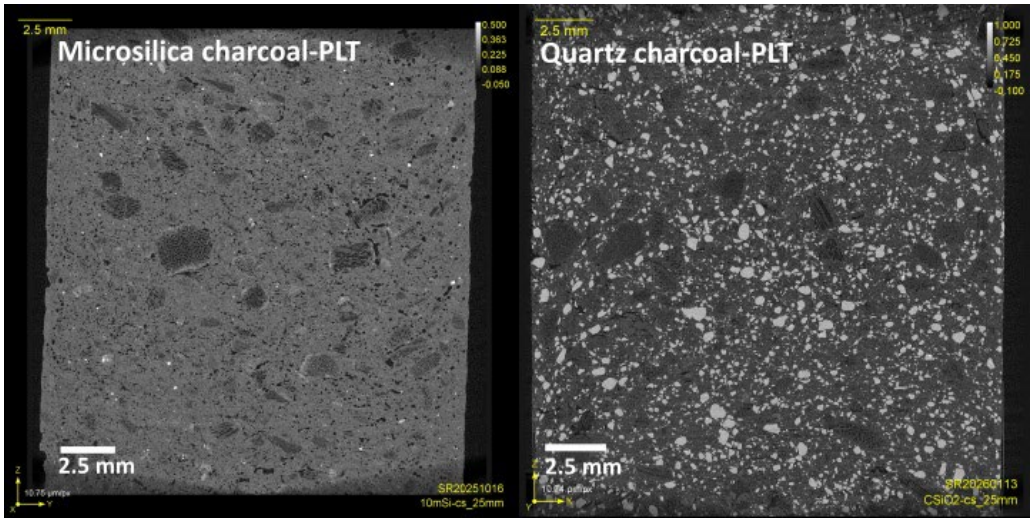

Figure 8. Extruded microsilica-carbon pellets and quartz-carbon pellets

Proximate analysis of the extruded pellets was performed at an accredited laboratory to determine the total fixed carbon (Fix-C), volatile matters and ash.

Table II: Proximate analysis of both the conventional carbon materials and the various agglomerated pellets.

Sample name	Fix-C (wt.%)	Volatiles (wt.%)	Ash (wt.%)	Moisture (wt.%)
Conventional carbon materials				
CK-009	87.08	0.61	11	4.5
CL-017	97.8	0.83	1.31	0.02
CC-016	91.9	3.18	3.67	1.27
CC-017	86.37	11.74	1.89	2.49
Agglomerated pellets				
10S-PLT	81.30	16.78	1.92	16.78
10SPL-PLT	75.69	12.71	11.6	1.01
10Ca-PLT	81.42	15.05	3.53	1.43
10Na-PLT	81.82	14.55	3.63	1.52
7SPL3S-PLT	81.91	15.85	2.24	0.91
7Ca3S-PLT	81.45	15.39	3.16	1.14
5SPL5S-PLT	81.42	16.24	2.34	0.90
5Ca5S-PLT	80.45	16.98	2.57	1.07
5Na5S-PLT	81.12	16.38	2.50	1.11

**CL-017, CC-016 and CC-017 proximate analysis measured after calcinated samples at 1200 °C.

2.3 Evaluating Mechanical Strength

Industrial furnaces are typically large and contain substantial amounts of raw materials. The production of dust and fines is closely correlated with the mechanical strength of these materials. Evaluating the cold strength is of importance as it both influences fines generation during transportation but also denotes the material's capacity to withstand the weight above it without undergoing crushing. Similarly, the interaction of carbon materials with gas and sudden temperature change upon entering the furnace can lead to a change in its strength (Monsen et al., 2007). The warm strength is the ability of the material to withstand the burden load of the descending charge materials and is measured through shock heating tests at the laboratory scale.

Cold Strength

The cold strength of carbon materials is a critical factor for various industries and currently represents a significant challenge in increasing the use of biocarbon. Studies have shown that up to 25% of charcoal can be lost during transport from the pyrolysis plant to the furnace, leading to substantial cost implications and potential environmental impacts due to the dispersal of fine particles **(Jahrsengene et al., 2023)**. Mechanical strength can be evaluated through multiple methods, each measuring different types of strength relevant to various stages of handling and processing. These methods include:

1. **Tumble/Drum test**: This measures resistance to abrasion and is the primary method used to estimate the degradation occurring during transport and furnace charging.
2. **Compression test**: This evaluates the breakage of materials under high loads, similar to those experienced in the lower parts of the furnace.

Tumble/Drum test

The strength of the sample was estimated by tumbling it in a rotating drum. Samples of approximately 100 g of either extruded pellets (maximum length 30–40 mm) or briquettes were tested separately in their original form without crushing. The selected sample was then placed in a steel drum with an inner diameter of 200 mm, equipped with four raisers spaced 90 degrees apart. A schematic illustration of the rotating drum used to evaluate the generation of fines is shown in Figure 9. The sample tumbled for a total of 30 min in two steps. In step 1, the sample tumbled for 10 min at 40 rpm. Then the sample was removed, sieved into size fractions of 10 mm, 6.3 mm, 4.75 mm, 3.35 mm, 1.25 mm, 0.5 mm, 0.25 mm, and 0.125 mm and the size distribution was measured. The entire sample was then placed back in the drum and tumbled for an additional 20 min at 40 rpm. After this second tumbling, the sample was removed and re-sieved. The fraction of fines, defined as any material under 3.35 mm, was used to determine the mechanical strength of the material. These methods ensure a comprehensive understanding of the mechanical durability of carbon materials, which is essential for optimizing its use in industrial processes and minimizing material losses and environmental impacts.

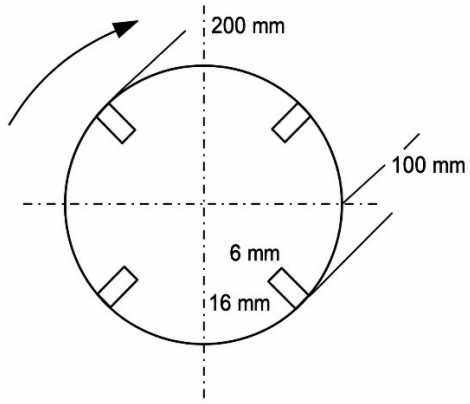

Figure 9. Schematic illustration of the rotating drum.

Compression Tests

Compression tests were conducted using a Zwick Roell compression tester with a maximum load capacity of 2500 N (Jayakumari and Ksiazek, 2024). Extruded pellets of 10 mm length were subjected to an increasing compression load until failure. The compression tester's head moved at a fixed rate of 2 mm/min, and the applied load was recorded. The test continued until either failure occurred or the original sample height was reduced by at least 4 mm. For

each carbon type (extruded pellets or briquettes), 10 tests were performed: 5 tests parallel to the extrusion direction and 5 perpendicular. The average, minimum, and maximum peak load for each direction were calculated.

Warm Strength (Thermal Shock Heating)

In industrial silicon furnaces, raw materials are subjected to rapid heating as the furnace's top typically reaches temperatures of 800–1000 °C. This rapid temperature change can induce significant thermal stresses, leading to the fracturing of the material. The ability of a carbon reductant to withstand this rapid heating is crucial for maintaining its integrity and performance in the furnace (Smith-Hanssen, Jahrsengene and Ringdalen, 2023b). This can be assessed using the Thermal Shock Heating test.

In this method, 100 g of a sample with a known particle size is dropped into a crucible preheated to 1000 °C and held at this temperature for 10 min. This test simulates the conditions for Si-production in a submerged arc furnace where cold fresh charge is introduced on top of the hot burden. The change in particle size distribution after exposure provides an indication of the material's thermal shock resistance. Following the test, the sample is sieved into the following size fractions: 10, 6.7, 4.75, 3.35, 1.25, 0.5, 0.25, and 0.125 mm. The aim of this task was to investigate the effect of fines generation in different reduction materials at temperature relevant to different furnace operations. Temperatures in the upper burden region of Mn alloys furnaces are typically below 500 °C, contrasting with temperature up to 1000 °C for Si furnaces (Ringdalen, 2014; Jusnes, 2020; Aasly Kurt , 2016). Therefore, the samples were subjected to thermal shock at both 500 °C and 1000 °C for 10 minutes to evaluate the influence of thermal shock under different temperature conditions. The resulting particle size distributions were then determined and compared to identify differences in material behaviour and test temperature.

Curing

The effect of curing was investigated on pellets samples made with two different recipes, one with only starch as the binder and another with a combination of Ca-lignosulphonate and starch. A muffle furnace capable of operating under argon atmosphere was used and the samples were heated to 200, 250 and 300 °C separately, with a holding time of 30 minutes at the final target temperature. After curing and for each temperature program, one pellet was immersed in water to assess the resistance to degradation, while the remaining samples were subjected to an abrasion (cold strength) test to evaluate the effect of curing on the generation of fines.

2.4 Reactivity with furnace gas at high temperatures

In silicon and ferroalloys production processes reactivity of carbon materials strongly influences both energy consumption and final metal yield. In the silicon process, reactivity refers to the ability of carbon materials to react with silicon monoxide (SiO) gas to form silicon carbide (SiC) which is the main intermediate compound in the final silicon forming reaction. Therefore, a carbon reductant with sufficiently high reactivity is required. In contrast, in the manganese process, the reactivity of carbon towards carbon dioxide (CO_2) gas is critical and undesired, as it affects the carbon balance and energy efficiency. In this case, a lower reactivity is preferred to minimize excessive carbon consumption (Schei, Tuset and Tveit, 1998; Olsen, Tangstad and Lindstad, 2026).

CO_2 – Reactivity test

The CO_2 reactivity test was performed using a thermogravimetric furnace (Figure 10), by a method developed by NTNU/SINTEF specifically for Mn alloy production. In the industrial manganese process, the CO_2 concentration ranges from 0 to 50%, and the temperature increases from the top of the charge towards the top of the coke bed where the liquid slag is formed (Olsen, Tangstad and Lindstad, 2026). The tests are conducted in an atmosphere that consists of either 75% CO and 25% CO_2 or 50% CO and 50% CO_2, simulating the conditions in the furnace, at temperatures ranging from 800 to 1100 °C (Jayakumari et al., 2023). In this work, a 50:50 ratio of CO:CO_2 and a temperature of 1100 °C were selected.

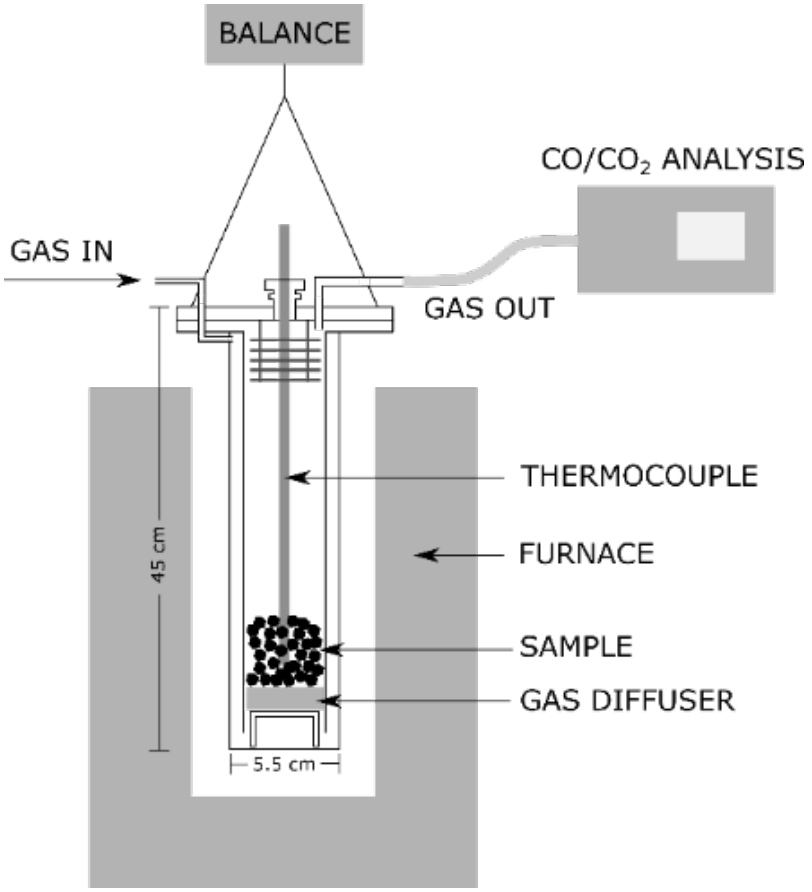

Figure 10. TGA furnace setup is used to measure the CO_2 reactivity (Jayakumari et al., 2023).

The test involves heating approximately 100 g of 5–10 mm carbon samples at a rate of 10 °C/min to reach a temperature of 1100 °C. The samples are then held at this temperature for 1 hr 45 min in a flow of 1 L/min of argon, followed by a flow of 4 L/min for an additional 30 min. Once the temperature reached 1100 °C, the Ar gas is replaced with a mixture of 50% CO and 50% CO_2 (2 L/min each). The weight change of the sample is continuously monitored to track the reaction between the carbon and CO_2 to produce CO. At 1100 °C, any volatiles and moisture are expected to be removed from the sample. As a result, any weight change observed during the experiment is solely due to the reaction between carbon and CO_2 to CO (Kaffash, Surup and Tangstad, 2021). The test is stopped when a weight loss corresponding to 20% of fixed carbon has reacted. The reaction of carbon results in a percentage mass loss curve that is linear with respect to time, and the slope of the curve corresponds to the CO_2 reactivity or the amount of fixed carbon (% fixed C) that reacts per unit time.

The strength of the materials depends on the extent of their reaction. It is therefore essential to examine the hot strength after the same degree of reaction, ensuring that the materials being compared are reduced by the same amount.

Thermal Abrasion Strength (warm strength)

The reaction of a carbon material with CO/CO_2 gas, along with gradual temperature changes when they descend in the furnace, can lead to a change in its strength. The ability of material to withstand abrasion after reaction is known as its **warm strength**. Loss of strength in carbon material due to their or binder reaction to gas can be measured. Here, the thermal abrasion test is performed on the reaction product obtained from the CO_2 reactivity test to measure the change or loss of strength in carbon material (Monsen et al., 2007). Prior to the test the carbon materials are first screened into specific size fractions.

To determine the thermal abrasion strength, the first step is to calculate the C.I (cohesion Index), which is the fraction of the largest size fraction (>4.75mm) after the CO_2 reactivity test (Monsen et al., 2007). Then, the sample is tumbled in a rotating drum (figure 9) for 10 min at 40 rpm, after which the sample is removed, sieved to 6.3, 4.75, 3.3 and 1.25 mm size fractions and the size distribution measured. The entire sample is placed back in the drum and tumbled for 20 more minutes at 40 rpm before being removed and re-sieved. The fraction of fines formed is reported from this test. In this case, the fraction of materials larger than 3.35 mm after tumbling is used to determine the T.I.3 (Thermal Stability Index), which represents the resistance to degradation and abrasion under furnace conditions.

SINTEF SiO reactivity test

The experimental set up for SINTEF SiO-reactivity tests consist of three separate alumina chambers heated by a graphite tube furnace (Tuset, J. K and Raaness, O., 1976; Lindstad et al., 2007b). The main reactions and distribution of gas flows through the SiO(g) generation chamber, reaction chamber and condensation chamber are illustrated in figure 11. The standard particle size range used for the test is 4–6.3 mm

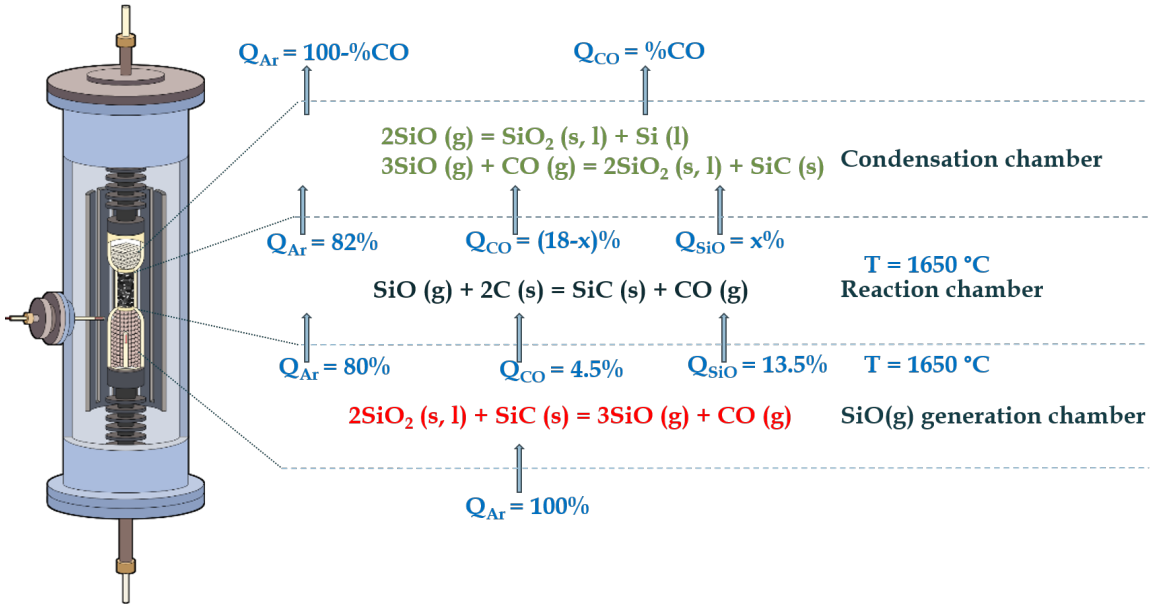

Figure 11. Schematic illustration of the experimental set up for SINTEF SiO reactivity test.

In the generation chamber, SiO(g) is generated at 1650 °C according to reaction 1 from pellets made of SiO_2 and SiC.

$2SiO_2 + SiC = 3SiO + CO$ (1)

The carbon materials, calcined before the test, are placed in the reaction chamber (the sample-bed with height 60 mm and radius 10 mm) which has a volume of 20 mL. During the test, SiO(g) passing though the carbon bed in the reaction chamber reacts to form SiC and CO (reaction 2). The SiO(g) left unreacted is captured and condensed in the condensation chamber. CO in the off gas is continuously measured.

$SiO + 2C = SiC + CO$ (2)

The gas from the generation chamber leaves saturated in SiO and CO. From equilibrium calculation at 1650 °C, this corresponds to a mixture of 13.5% SiO, 4.5% CO and 82% Ar (Lindstad et al., 2007b). When SiO(g) reacts with carbon materials, CO is generated: full conversion of SiO to SiC results in an outlet gas containing 18% CO. When CO drops down to 6%, it indicates that nearly all SiO(g) passes unreacted through the carbon material in the reaction chamber and condenses at the condensation chamber according to reaction 3 and 4.

$2SiO = SiO_2 + Si$ (3)

$3SiO + CO = 2SiO_2 + SiC$ (4)

The time taken for the concentration of CO to decrease from 18% to 6% depends on the properties of the carbon materials. Thus, the reactivity is defined as the volume of SiO(g), in mL, which passes through the carbon layer in the time in which CO decreases from 18% to 10% (R10) or to 6% (R6) as calculated from the equations below (Lindstad et al., 2007b).

$$R10 = \sum_{18\rightarrow 10\%} \frac{Q_{Ar}(18 - \%CO)}{82 - 0.82 * \%CO} * \Delta t$$

$$R6 = \sum_{18\rightarrow 6\%} \frac{Q_{Ar}(18 - \%CO)}{82 - 0.82 * \%CO} * \Delta t$$

3. RESULTS AND DISCUSSION

The results and discussion are mainly divided into two parts: mechanical strength and reactivity. The mechanical strength of the agglomerated materials was evaluated using several methods described in section 2. In addition, the reactivity of the materials was investigated, focusing on CO_2 and SiO reactivity.

3.1 Cold strength

Figure 1, presents the cold strength results for agglomerated pellets and briquettes produced with different binder compositions, along with charcoal (CC-17) and coke (CK-009).

Seven different briquettes (BRQT) and eleven different charcoal pellets (PLT) produced using different binder compositions were selected for the cold strength measurements. Interestingly, pellets made using starch as a binder generate a low amount of fines (<10%) after 30 min of tumbling, comparable to the fines produced by coke (<10%). In contrast, the highest fines generation is observed for pellets produced with SPL as a binder (50 – 80%). As indicated by the CT images, pellets made with SPL exhibit a cracked structure, which weakens the material and leads to increased fines formation. In the case of briquettes, fines generation remains relatively high and shows little variation across different compositions. Among the tested samples, starch-based agglomerates consistently produce the lowest amount of fines.

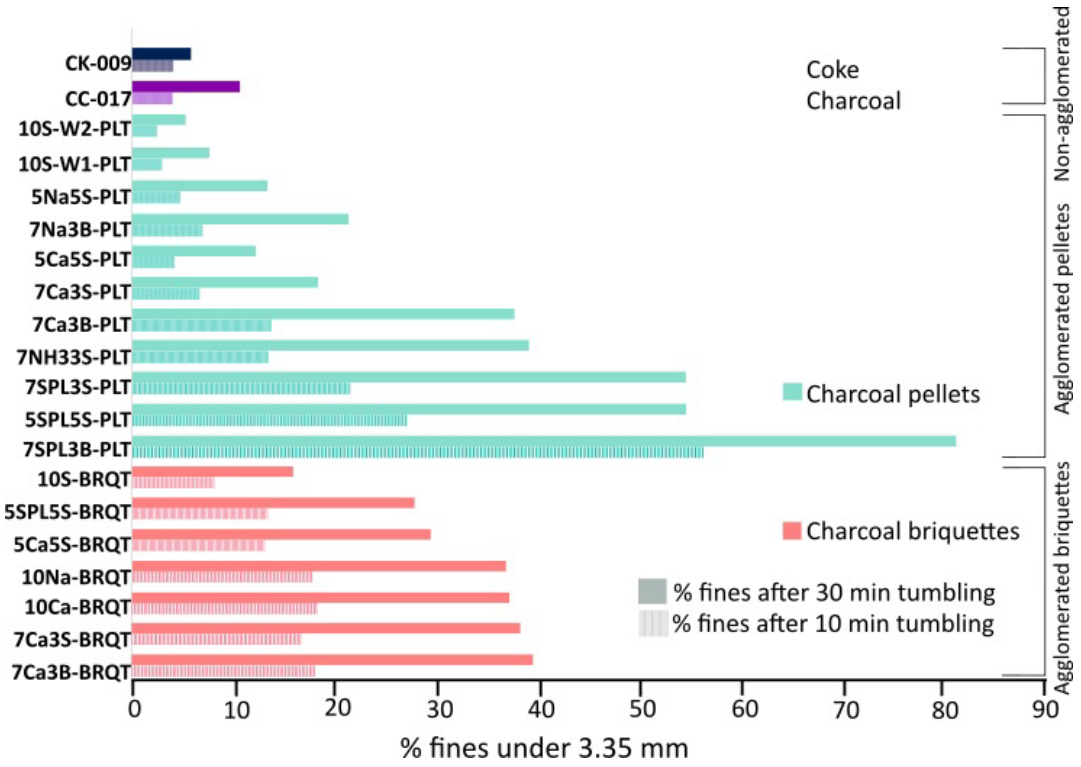

Figure 11. The cold strength results for agglomerated pellets and briquettes produced with different binder compositions, along with charcoal (CC-17) and coke (CK-009). W1 and W2 denote pellets prepared with same binder, differing only in the amount of water used during pelletization.

3.2 Compression strength

To evaluate the effect of furnace conditions on pellet strength, compression tests were performed on pellets both before and after exposure to CO/CO_2 atmosphere at 1100 °C. All pellets had approximately the same dimensions, with a diameter of 15 mm and a length of 15 mm. The results are summarized in Figure 12 and 13, which presents the average peak load for all samples, along with the corresponding minimum and maximum values measured for each type of extruded pellet. In both conditions, pellets produced using starch as a binder exhibit the highest strength, with maximum forces in the range of 1200–1800 N. In contrast, pellets made with SPL show the lowest initial strength (figure 12). However, an increase in strength (figure 13) is observed for SPL-based pellets after exposure to elevated temperature and reactive gas, indicating structural changes during heat treatment. The increase in strength of SPL-based pellets after heat treatment can be attributed to thermal densification and sintering, which enhance inter-particle bonding and reduce pore volume, as reported in previous studies (Chhiti et al., 2012; Branca and Di Blasi, 2025; Pahnila et al., 2026). Previous studies indicate that lignin exhibits thermoplastic behaviour at moderate temperatures, enhancing particle bonding. However, at higher temperatures it undergoes thermal decomposition and carbonization, forming a more rigid carbon structure that can contribute to increased strength after heat treatment (Chhiti et al., 2012). Overall, starch-based pellets exhibited the highest mechanical strength both before and after exposure to furnace conditions.

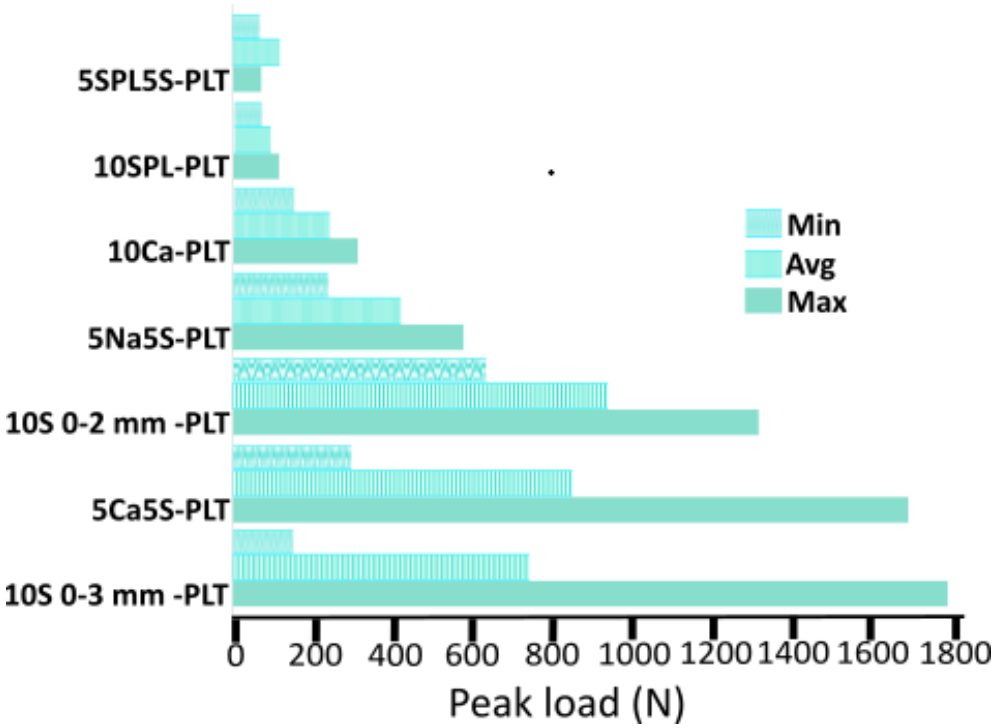

Figure 12. Force at failure in compression test for untreated pellets.

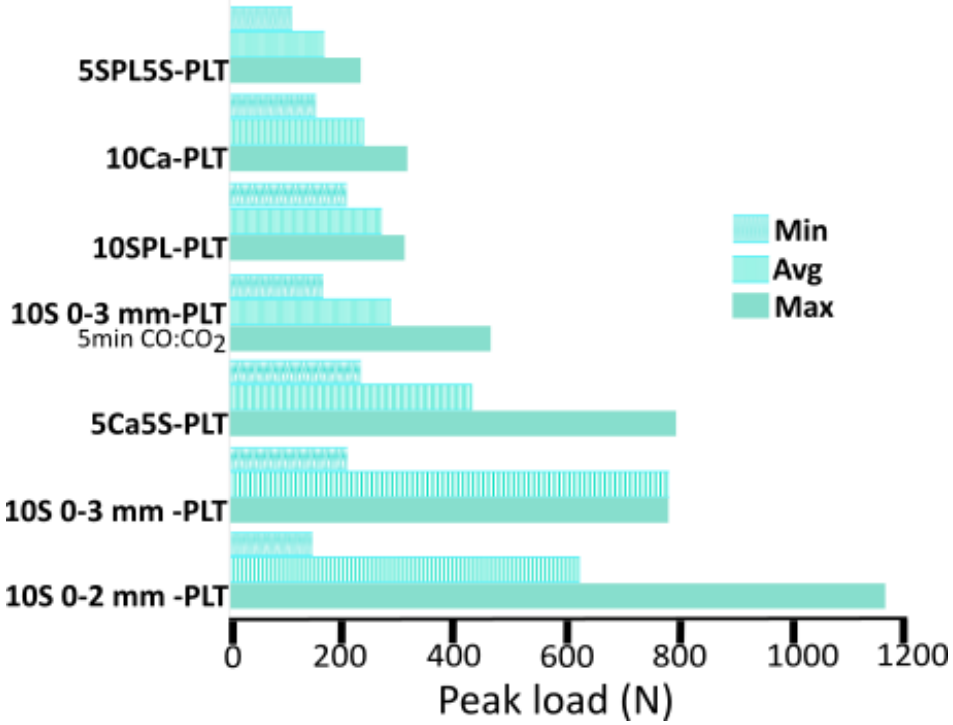

Figure 13. Force at failure in compression test for pellets exposed to CO/CO_2.

3.3 Curing

Figure 14 illustrates the behaviour of various pellets after curing and water exposure for 30 min, 1 h or 24 h. Pellets heat-treated at 200 °C showed poor resistance to water, with disintegration initiating immediately as charcoal fines began to separate, leading to complete dissolution within 1 h. In contrast, pellets cured at 250 °C remained intact in water without noticeable decomposition even after 24 h. A similar behaviour was observed for pellets treated at 300 °C. These results indicate that curing in the temperature range of 250-300 °C is necessary to strengthen the binder network and improve water resistance.

Previous studies have shown that elevated temperatures activate lignosulphonate, enhancing its binding strength (Borregard, n.d.). For example, refractory materials bonded with lignosulphonate are typically cured at 180-220 °C, where the lignin-based binder undergoes activation and improves mechanical integrity. Furthermore, thermal treatment at higher temperatures can lead to carbonization under inert or reducing conditions, contributing to stronger inter-particle bonding. Even under oxidizing conditions, lignin oxidizes relatively slowly, allowing partial char formation if the treatment duration is carefully controlled.

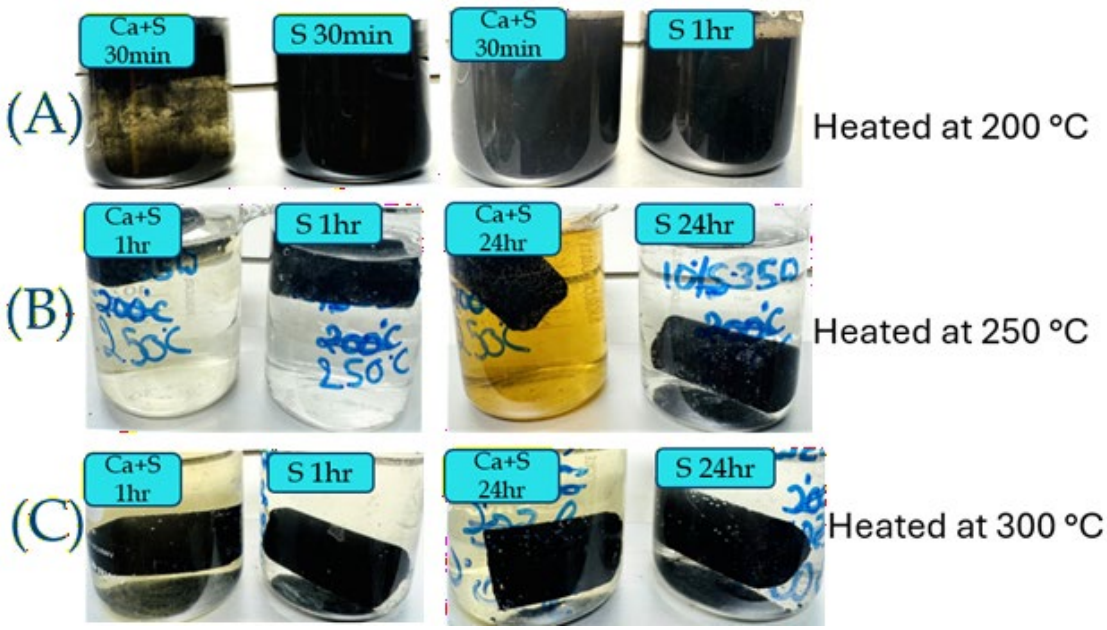

Figure 14. The behaviour of various pellets after curing and water exposure for 30 min, 1 h or 24 h.

The same pellets cured at the three different temperatures were also subjected to a tumbling test. Interestingly, after 30 min of tumbling, pellets cured at 300 °C generated a larger amount of fines, followed by those cured at 250 °C and 200 °C, as shown in figure 15. This suggests that although higher curing temperatures improve water resistance, excessive thermal treatment may lead to increased brittleness, resulting in higher fines generation under mechanical stress. The higher fines generation observed for pellets cured at 300 °C can be directly related to changes in binder chemistry and resulting brittleness. At moderate temperatures (200-250 °C), binders such as starch and lignosulphonate undergo thermal activation and partial cross-linking, which improves inter-particle bonding while still retaining some flexibility in the structure. However, at 300 °C, further heating leads to advanced decomposition and carbonization of the binder, resulting in a more rigid and brittle network. This over-carbonization reduces the ability of the binder to absorb mechanical stress, making the pellets more prone to fracture during tumbling. In other words, while curing at higher temperature improves water resistance and compressive strength, it simultaneously reduces toughness, leading to increased fines generation under dynamic conditions. This could be the reason why pellets cured at 300 °C produced more fines compared to those cured at 250 °C and 200 °C.

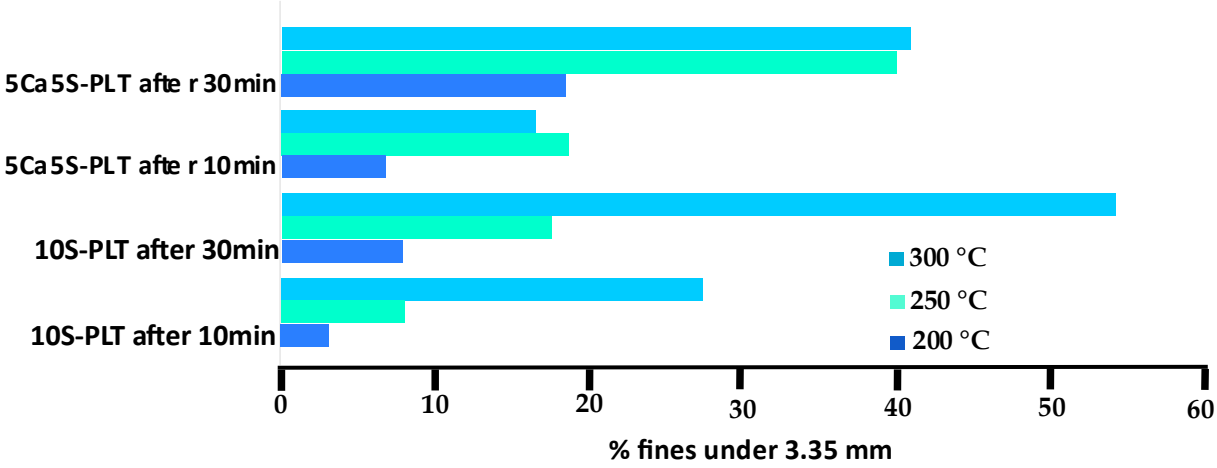

Figure 15. Fines generation during tumbling for samples cured at 200, 250 and 300 °C.

3.4 Thermal Shock Heating

Shock heating tests were performed on laboratory-produced extruded pellets to evaluate fines generation during rapid heating, simulating conditions encountered when materials enter the furnace at approximately 1000 °C. Figure 16 illustrates the cumulative size distribution (percentage passing each sieve) of the pellets after shock heating and 10 min holding at the temperature. The fraction of fines, defined as particles smaller than 3.35 mm, was used as an indicator of mechanical strength. Figure 16 highlights the cumulative percentage below 3.35 mm.

A total of 19 pellets recipes, prepared with different binders and combination of binders, were selected for the test. After sieving, all samples generated less than 5% fines, indicating good resistance to thermal shock-induced disintegration. Similarly, Figure 17 presents the size distribution for four selected briquette samples after shock heating. These briquettes produced even lower fines fractions, below 1% for particles under 3.35 mm. The results demonstrate that both pellets and briquettes exhibit high structural stability under rapid exposure to elevated temperatures (1000 °C), suggesting that they would not undergo significant fragmentation upon entering the furnace. The appearance of the agglomerates after test is shown in Figure 18. While evaluating thermal shock at 1000 °C is relevant to Si production, the furnace top in Mn alloy processes do not reach similar temperatures. Figure 18 shows pellets after shock heating at 500 °C: negligible degradation is observed. This supports customization of these tests for each process.

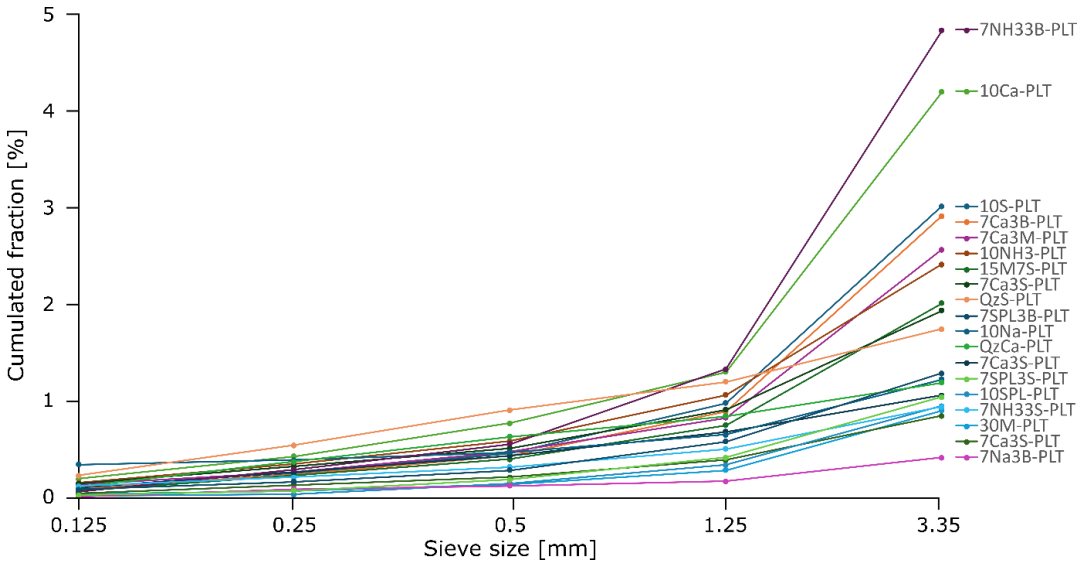

Figure 16. Distribution of fines after shock heating of pellets at 1000 °C.

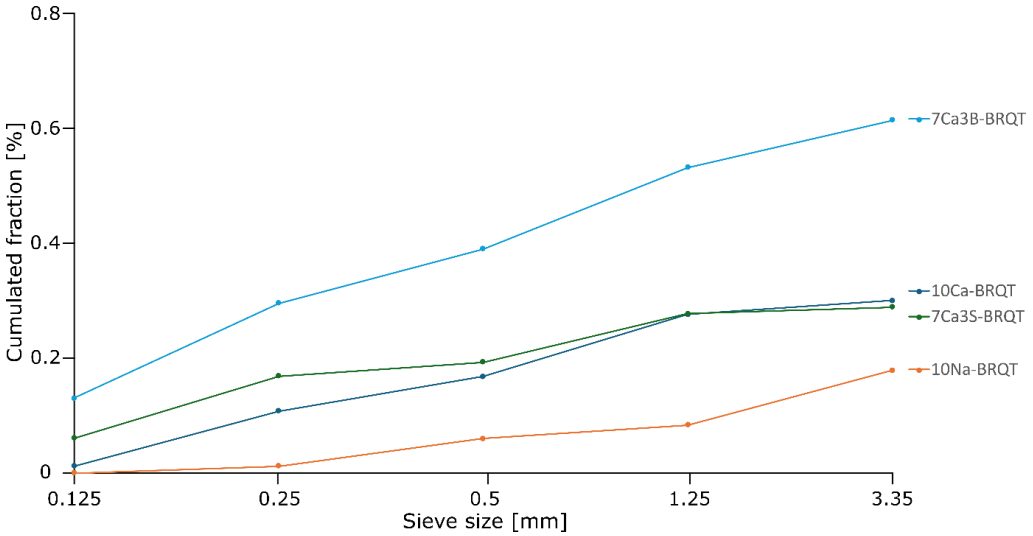

Figure 17. Distribution of fines after shock heating of briquettes at 1000 °C.

Figure 18. Visual aspect of pellets and briquettes after shock heating at 1000 °C.

Figure 19. Visual aspect of pellets after shock heating at 500 °C.

3.5 CO_2 reactivity

CO_2 reactivity tests were conducted on various agglomerated charcoal pellets and briquettes, charcoal, coal, and coke to evaluate their behaviour in a CO/CO_2 atmosphere. In addition, carbon black pellet samples (CB-1, CB-2, CB-3, and CB-4) were also tested. The primary difference among the carbon black samples lies in their composition: CB-1, CB-3, and CB-4 were produced from the same carbon black type with different binder compositions, whereas CB-2 was produced using a different carbon black type. Further details are not disclosed due to confidentiality (see Section 2.1). The results of the tested samples are summarized in figure 20, which presents the CO_2 reactivity of each material expressed as the percentage of fixed carbon (Fix-C) reacted per minute. The calculation of reactivity requires knowledge of the initial fixed carbon content of each sample (Table II). The results show that the biocarbon based

agglomerated pellets and briquettes exhibit CO_2 reactivity values within the same range as coal (CL-017). In contrast, the carbon black pellets demonstrate even lower reactivity than the biocarbon agglomerates. A notable variation is also observed within the carbon black samples, where CB-2 shows significantly lower reactivity compared to the other CB samples produced from the same carbon black type. For comparison, conventional carbon materials were also tested. As expected, charcoal exhibits the highest reactivity, followed by coal and then coke, which is consistent with differences in carbon structure and porosity. In general, the results indicate that while raw charcoal exhibits high CO_2 reactivity, agglomeration of biocarbon can effectively reduce its reactivity to levels comparable to fossil-based carbon such as coal. This highlights the potential of agglomeration processes to tailor the reactivity of biocarbon materials for industrial applications (Monsen et al., 2007; Jayakumari et al., 2023)

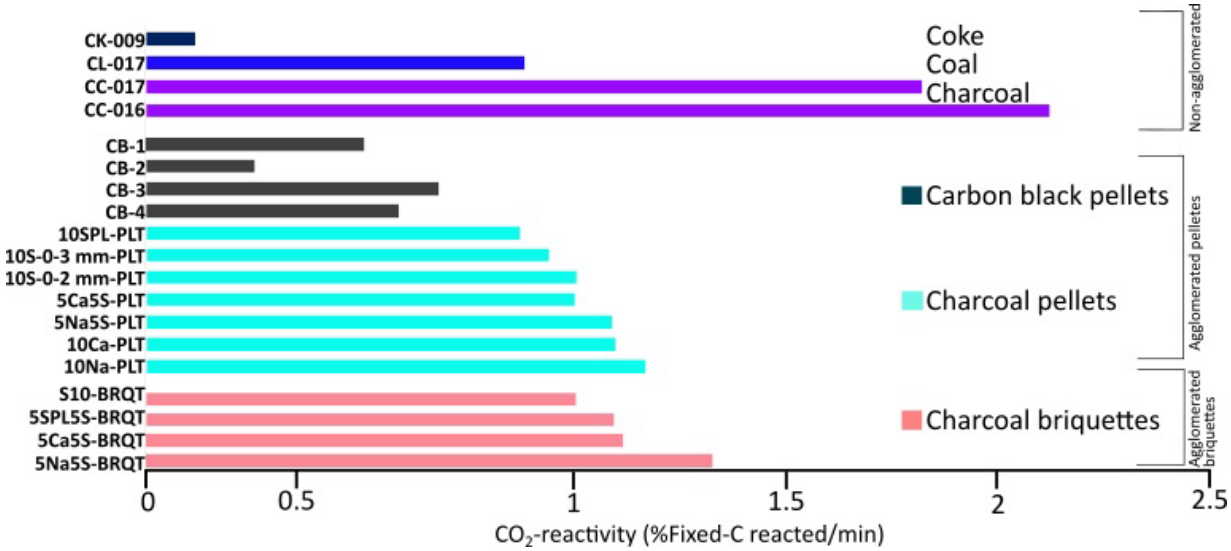

Figure 20. The CO_2 reactivity of each material expressed as the percentage of fixed carbon (Fix-C) reacted per minute.

A visual assessment of the samples was carried out before and after the CO_2 reactivity test, as shown in figure 21. After testing, most samples exhibited degradation primarily at the surface, where the outer layer appeared to be covered with carbon fines, while the internal structure remained relatively intact and hard. This suggests that the reaction was largely limited to the external regions of the pellets.

To verify this observation, one experiment was interrupted after heating the sample in an Ar atmosphere, just before introducing the CO/CO_2 gas mixture (figure 21). Interestingly, no visible changes were observed in the pellet before and after heating under inert conditions. This confirms that the gas-solid reaction predominantly occurs at the surface of the pellets rather than within the bulk.

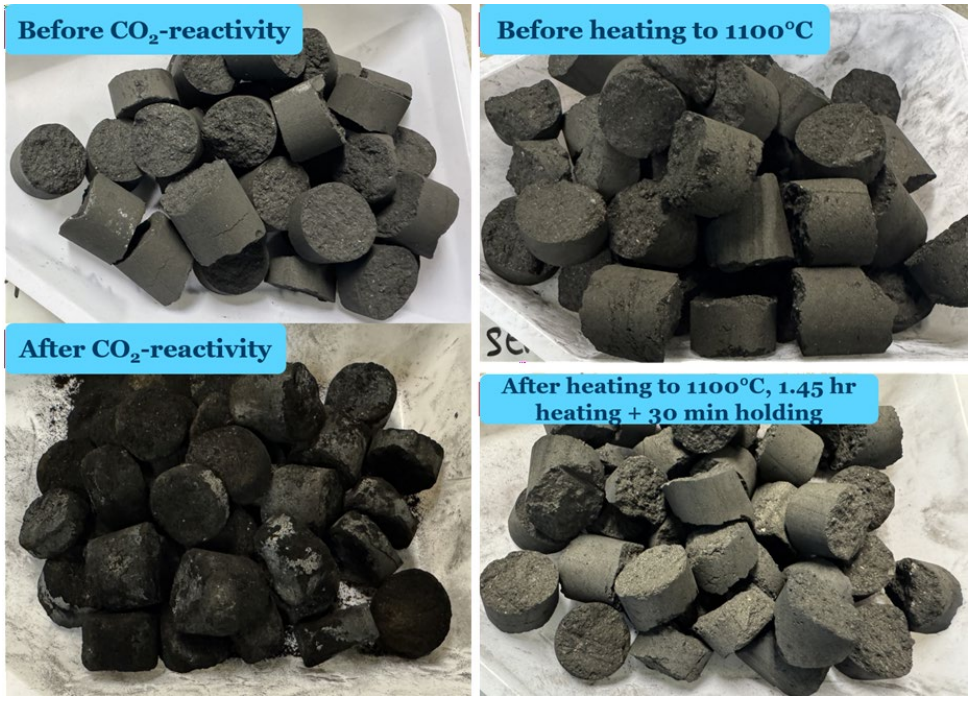

Figure 21. The appearance of sample before and after the CO_2 reactivity test and before and after heating 2 h 15 min at 1100 °C.

3.6 Warm strength after CO_2 reactivity

The warm strength discussed in this study refers to the mechanical integrity of carbon materials after exposure to CO_2 reactivity conditions and represents their abrasion resistance following reactions in a CO/CO_2 gas atmosphere, illustrating what happens in the pre-reduction zone of Mn furnaces. The strength of the samples is evaluated using the cohesion index (C.I.) and the thermal stability index (T.I.3). The C.I. is defined as the fraction of material larger than 4.75 mm after the CO_2 reactivity test, prior to any further handling, and provides an indication of the material's resistance to fines generation under furnace conditions.

Figure 22 presents the investigated samples along with their corresponding C.I. values. Most of the samples exhibit high C.I. values in the range of 80 - 98%, indicating strong resistance to degradation after exposure to reactive gas environments. Such high values are desirable, as they suggest that the materials can maintain their structural integrity during furnace operation.

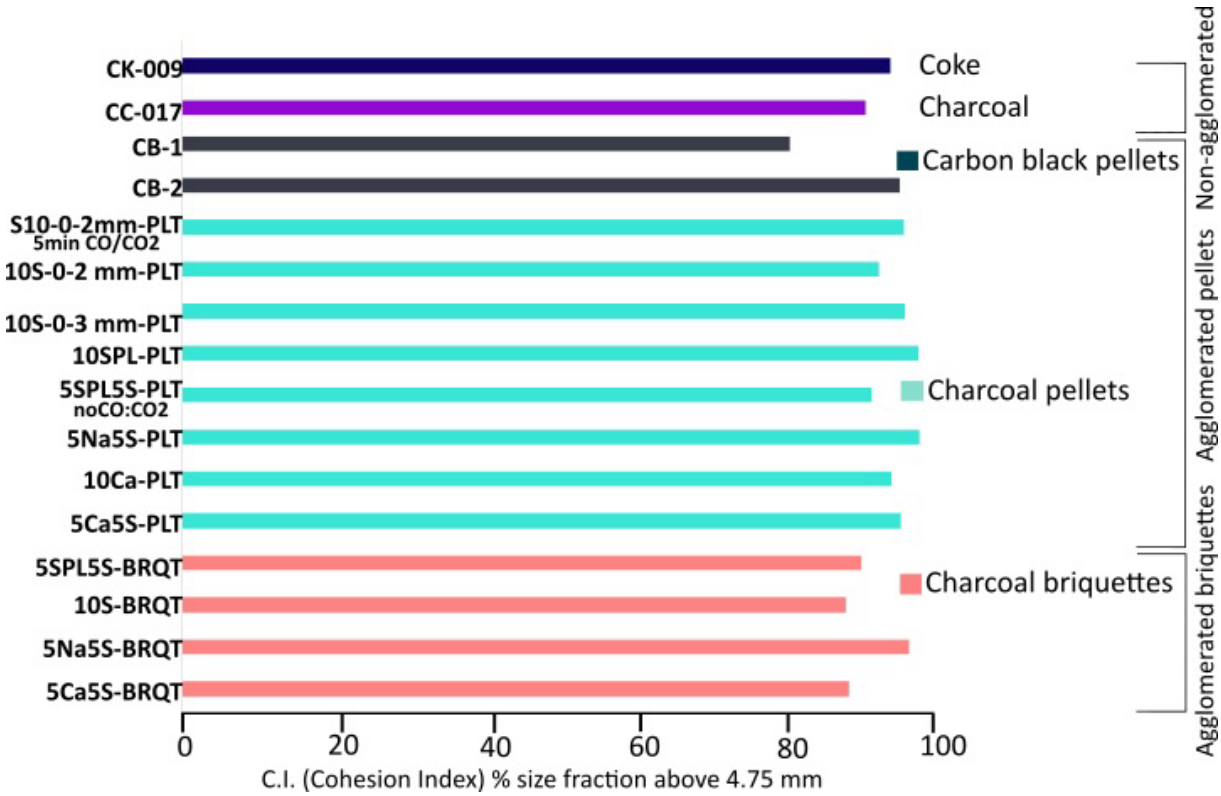

Figure 22. C.I (cohesion index) measured after CO_2 reactivity tests.

The thermal stability index (T.I.3) is defined as the fraction of material larger than 3.35 mm after the CO_2 reactivity test followed by tumbling in a rotating drum. It reflects how the Boudouard reaction influences the abrasion resistance of the materials, where a higher T.I.3 value is preferred. Figure 23 summarizes the T.I.3 values for all samples after 10 and 30 minutes of tumbling. A decrease in T.I.3 is observed for all samples with increasing tumbling time, indicating progressive degradation under mechanical stress. The reduction is more pronounced for the briquettes, where a significant drop in T.I.3 occurs between 10 and 30 minutes.

Among the tested materials, CB-1 pellets exhibit relatively high T.I.3 values, indicating good resistance to degradation, whereas CB-2 pellets were completely disintegrated into fines even after 10 minutes of tumbling. The substantial generation of fines after tumbling suggests that these samples experienced a considerable loss of structural integrity following the CO_2 reaction. In contrast, the conventional carbon materials charcoal, coal, and coke largely retained their mechanical strength after tumbling.

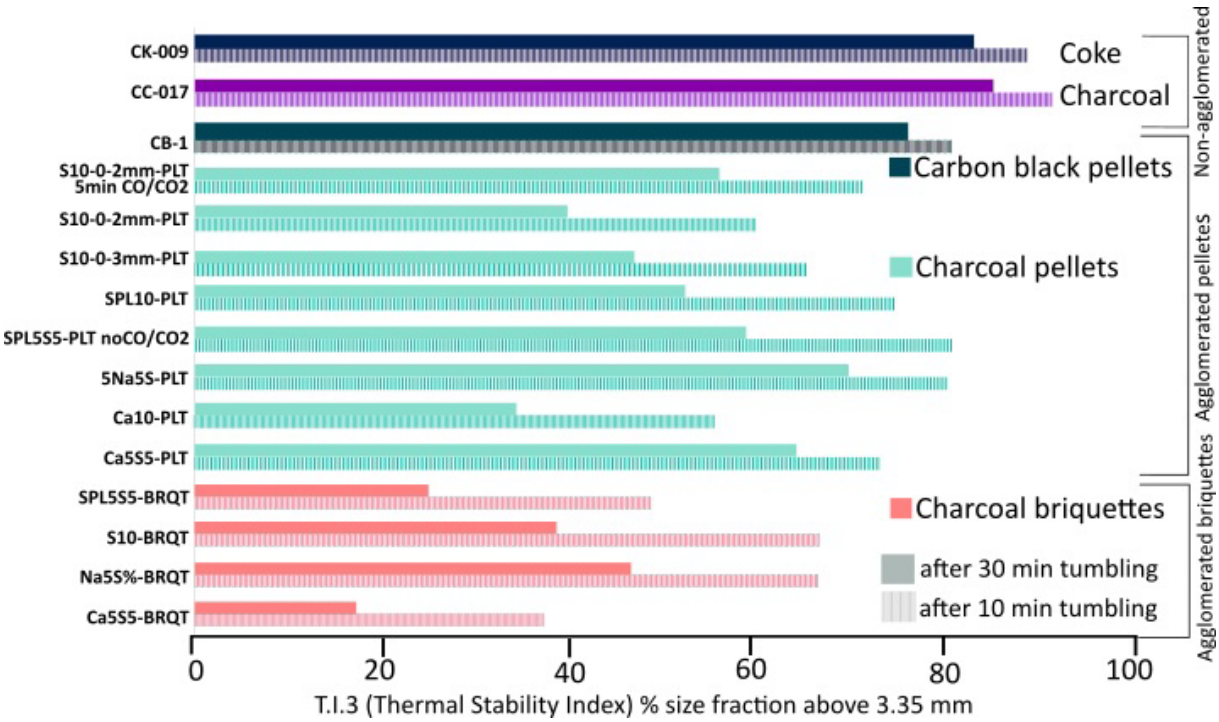

Figure 23. T.I.3 (thermal stability index) measured after CO_2 reactivity test.

3.7 SiO reactivity

The SiO reactivity test measures the ability of a carbon sample to react with SiO gas to form SiC and is expressed as R10. The R10 value is reported in terms of the volume of SiO, where a higher R10 indicates lower reactivity (slower reaction with SiO gas) (Lindstad et al., 2007b). Selected biocarbon agglomerates, carbon black pellets, and conventional carbon materials were subjected to this test, R10 values are shown in Figure 24.

Compared to raw charcoal, the charcoal-based pellets generally exhibit slightly lower reactivity, reflected by higher R10 values. Among the charcoal pellets, those produced with 100% starch and with a 50:50 combination of starch and lignosulphonate binders show higher R10 values compared to pellets made with SPL, Ca-, and NH_4-lignosulphonates, except for Na-lignosulphonate. Consistent with observations from other tests, differences are also seen among the carbon black samples: CB-1 shows slightly lower R10 values (higher reactivity) compared to CB-2, indicating that the type of carbon black significantly influences reactivity.

For reference, conventional carbon materials including charcoal sources (CC-017 and CC-016), coal (CL-017), and coke (CK-009) were also tested. As expected, charcoal exhibits the highest reactivity, followed by coal and then coke. Reproducibility was verified through parallel tests on CL-017 and selected carbon black samples, and average R10 values were used for evaluation. An additional test on CB-2 with a narrower size fraction (4-4.75 mm) showed no significant variation in reactivity. In general, all agglomerated pellets except CB-2 exhibit reactivity values within the range of charcoal to coal, as illustrated in the reactivity scale (Figure 25).

Overall, the results suggest that both SiO and CO_2 reactivity are closely linked to the pore structure of the materials, where higher porosity promotes greater gas accessibility and thus higher reactivity, while agglomeration reduces porosity and moderates reactivity toward levels comparable to conventional carbon materials (Jayakumari and Ringdalen, 2022).

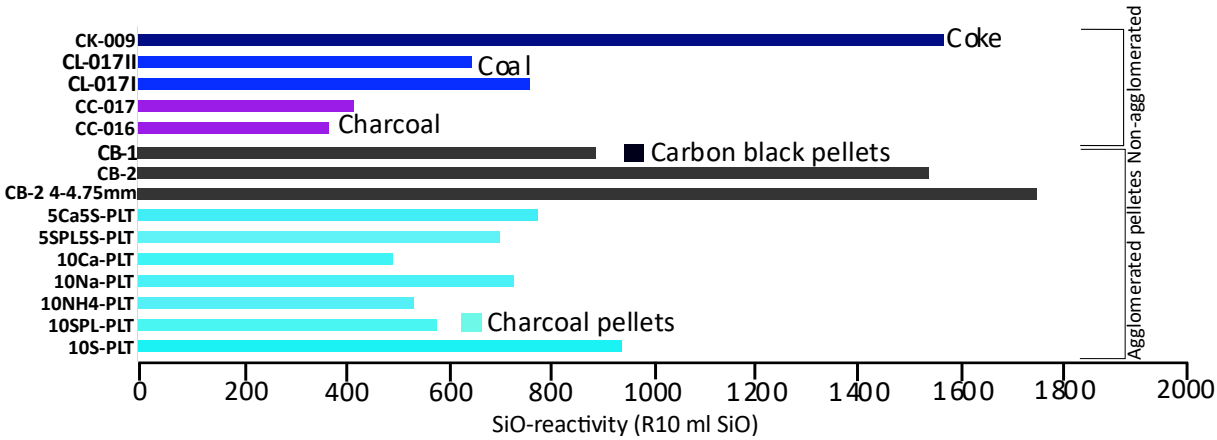

Figure 24. R10 reactivity measured in ml SiO for all the tested carbon samples.

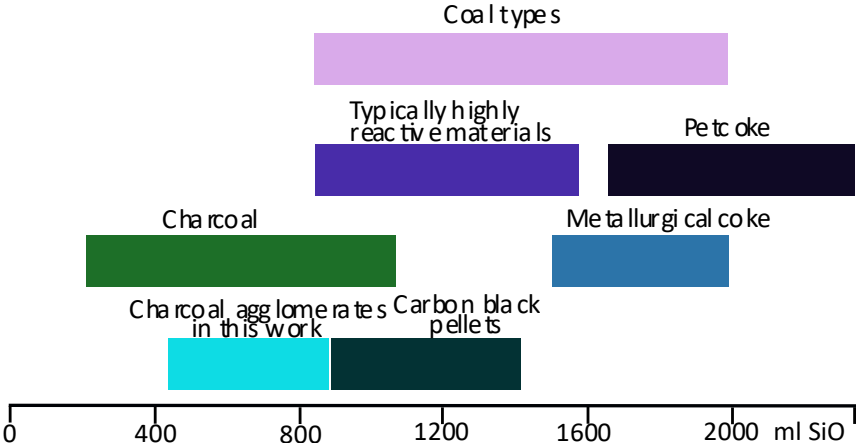

Figure 25. SiO-reactivity of different carbon reductants measured with SINTEF SiO-reactivity test and reactivity values of the agglomerated carbon materials from the current study is also included (Jayakumari and Ringdalen, 2022).

Figure 26 presents CT images of calcined pellets in the size range of 4–6.3 mm (A), partially converted SiC particles (B), and fully converted SiC particles (C), illustrating the transformation behaviour when carbon pellets react with SiO gas. These observations provide insight into the diffusion-controlled mechanisms governing the reaction of SiO gas within agglomerated particles.

In Figure 26 (A), the calcined pellets prior to the SiO test appear relatively dense, with a heterogeneous distribution of coarse and fine particles. In Figure 26 (B), the partially converted samples show grey regions corresponding to SiC formation, while darker regions represent unreacted carbon. The conversion pattern seems to follow the shrinking core model (SCM), where the reaction initiates at the surface of the particle, forming an outer SiC layer that gradually thickens as the reaction proceeds. As described by Schei et al. (Schei, Tuset and Tveit, 1998), the reaction rate decreases with increasing SiC layer thickness, due to the need for SiO(g) to diffuse through this layer to reach the unreacted carbon core.

The present observations confirm that the SCM adequately describes the transformation of charcoal-based agglomerates from carbon to SiC, consistent with previous findings for charcoal (Jayakumari, 2020). However, coal and pet-coke samples exhibit different behaviour and do not strictly follow the SCM mechanism, indicating differences in pore structure and reaction pathways. Previous studies on the kinetics of SiO–carbon reactions also support such material-dependent behaviour (Myrhaug, n.d.,2003).

In Figure 26 (C), the particles are fully converted to SiC, with no remaining unreacted carbon, indicating that SiO gas diffusion is not significantly hindered within the agglomerated structure. This can be attributed to the inherently high porosity of charcoal, characterized by

thin cell walls, which facilitates gas diffusion and promotes complete conversion. Since the agglomerates in this study are produced from charcoal fines, the results demonstrate that agglomeration does not significantly impede SiO diffusion or SiC formation.

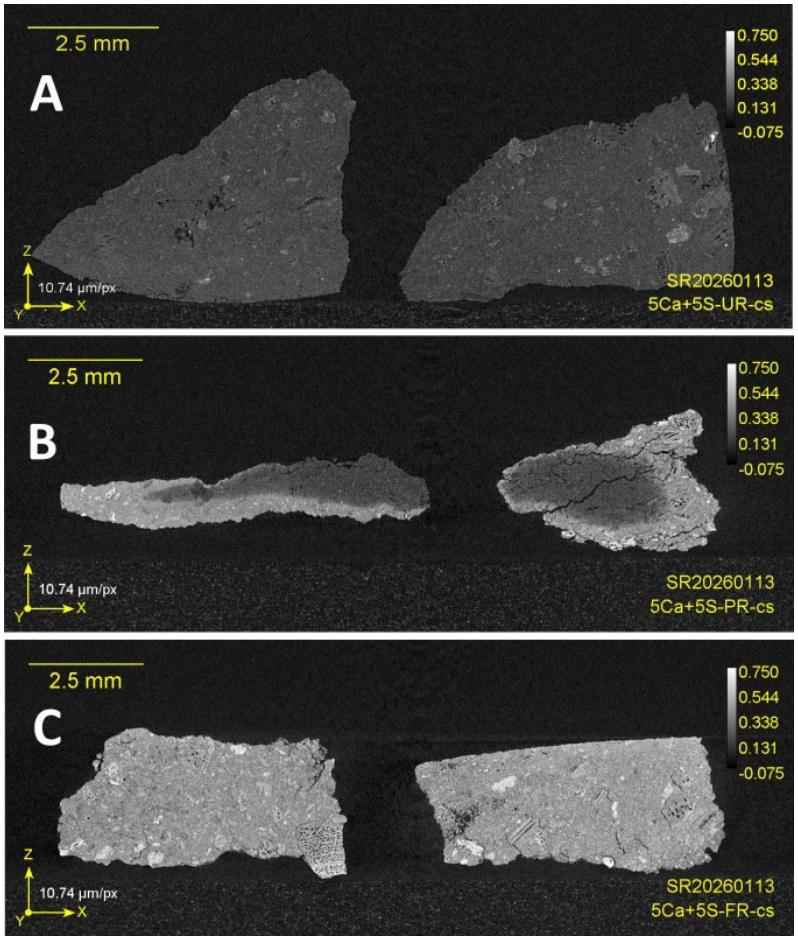

Figure 26. CT of pellets A. unreacted, B. partially reacted and C. Fully reacted to SiC.

Carbon weight gain

At 100% conversion, one mole of SiC is formed from two moles of carbon according to the reaction;

$$SiO(g) + 2C\ (s) = SiC\ (s) + CO\ g)$$

This reaction takes place in the reaction chamber where the carbon particles are located. Based on stoichiometry, 2 moles of carbon (2 x 12.01 g = 24.02 g) form 1 mole of SiC (28.09 + 12.01 = 40.01 g). The theoretical mass increase factor is therefore:

$$\frac{M_{SiC}}{2M_C} = \frac{40,1}{2 \cdot 12,01} = 1,6694 \approx 1,67$$

If a carbon material does not contain ash at all, the theoretical weight gain at full conversion will be 66.9 ≈ 67%. Consequently, the degree of conversion can be estimated directly from the mass increase relative to the theoretical maximum of 67%. The percentage of SiC conversion calculated from the mass gain after the SiO reactivity test for various agglomerated pellets and conventional carbon materials are summarized in Figure 27. The results show that all tested materials, including both agglomerated and conventional carbon samples, achieved SiC conversion levels above 80%, except for coke (CK-009). This indicates that the agglomerated pellets retain a high capacity for SiC formation despite the agglomeration process.

Furthermore, the high conversion levels suggest that SiO gas can effectively diffuse into the agglomerated particles and react with the carbon, resulting in extensive SiC formation.

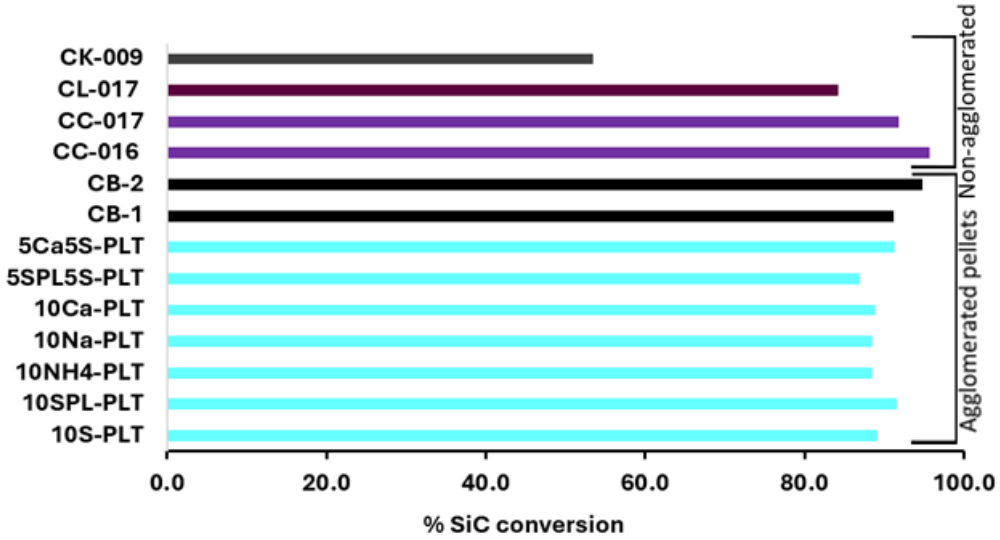

Figure 27. The percentage of SiC conversion calculated from the mass gain after the SiO reactivity test for various agglomerated pellets and conventional carbon materials.

4. CONCLUSIONS

In this study, biocarbon agglomerates in the form of extruded pellets and briquettes produced with different binder compositions were investigated with respect to their physical properties, mechanical strength, thermal stability, and reactivity. The results showed that agglomeration produced materials with a more homogeneous structure, higher bulk density, and lower porosity than raw charcoal. Among the investigated binders, starch-based agglomerates exhibited the highest cold and warm strength, while SPL-based pellets showed improved strength after heat treatment. Both pellets and briquettes demonstrated good resistance to thermal shock, generating only limited amounts of fines after exposure to elevated temperatures.

Furthermore, agglomeration reduced the CO_2 and SiO reactivity of the biocarbon materials to levels comparable to coal, while maintaining high SiC conversion (>80%) in most samples. Overall, the results demonstrate that charcoal fines can be successfully agglomerated into mechanically robust and thermally stable materials with properties suitable for ferroalloy production processes.

5. ACKNOWLEDGEMENTS

This work was carried out through a collaboration between the SINTEF-funded *Forskerinitierte strategiske egnefinansierte prosjekter* (SEP) 2025 initiative and the MECALO project, funded by the EU Horizon Europe programme (Grant Agreement No. 101177480). The Views and opinions expressed herein are those of the author(s) only and do not necessarily reflect those of the European Union or HADEA. Neither the European Union nor the granting authority can be held responsible for them. The support and contributions of both projects are gratefully acknowledged.

We would also like to express our sincere gratitude to Hugo Letartre for his immense contribution to the agglomeration work and various laboratory activities during his internship period with our team. His dedication and valuable support are highly appreciated. All contributions and funding sources are gratefully acknowledged.

6. REFERENCES

Aasly Kurt and, D.V., June 13 - 16, 20016. *Assessment of production performance of quartz in the Si-furnace*.

Borregard, n.d. *TRANSFORMING WASTE INTO VALUE WITH SUSTAINABLE BINDERS.*

Branca, C. and Di Blasi, C., 2025. Packed-Bed Pyrolysis of Alkali Lignin for Value-Added Products. *Recycling*, 10(2), p.66. https://doi.org/10.3390/recycling10020066.

Butler, J.W., Skrivan, W. and Lotfi, S., 2023. Identification of Optimal Binders for Torrefied Biomass Pellets. *Energies*, 16(8), p.3390. https://doi.org/10.3390/en16083390.

Chhiti, Y., Salvador, S., Commandré, J.-M. and Broust, F., 2012. Thermal decomposition of bio-oil: Focus on the products yields under different pyrolysis conditions. *Fuel*, 102, pp.274–281. https://doi.org/10.1016/j.fuel.2012.06.098.

Han, Y. and Tangstad, M., 2024. Metallurgical Properties of Biocarbon in Ferroalloy Production─A Review. *ACS Omega*, 9(23), pp.24142–24162. https://doi.org/10.1021/acsomega.4c00866.

Hoover, H., Bell, R. and Rippy, K., 2024. Emerging Technologies for Decarbonizing Silicon Production. *Journal of Sustainable Metallurgy*, 10(4), pp.1921–1932. https://doi.org/10.1007/s40831-024-00913-3.

Jahrsengene, G., Jayakumari, S., Kero, I.T. and Ringdalen, E., 2023. Sustainable Metal Production: Use of Biocarbon and the Concern of Dusting. In: Metallurgy and Materials Society of the Canadian Institute of Mining Metallurgy and Petroleum (CIM), ed. *Proceedings of the 62nd Conference of Metallurgists, COM 2023*. [online] Cham: Springer Nature Switzerland. pp.1001–1007. https://doi.org/10.1007/978-3-031-38141-6_126.

Jayakumari, S., 2020. *Formation and characterization of β-and α-Silicon Carbide produced during Silicon/Ferrosilicon process*. [online] NTNU. Available at: <https://ntnuopen.ntnu.no/ntnu-xmlui/handle/11250/2678922> [Accessed 21 November 2021].

Jayakumari, S., Jahrsengene, G., Ksiazek, M. and Ringdalen, E., 2023. Investigations on CO2 Reactivity and Thermal Strength of Carbon Sources for Ferroalloy and Silicon Production. In: *Proceedings of the 62nd Conference of Metallurgists, COM 2023*. [online] Conference of Metallurgists. Springer, Cham. pp.1009–1018. https://doi.org/10.1007/978-3-031-38141-6_127.

Jayakumari, S. and Ksiazek, M., 2024. *Fines Generation and Strength of Various Carbon Materials Used in the Ferroalloy Industries*. https://doi.org/10.2139/ssrn.4942468.

Jayakumari, S. and Ringdalen, E., 2022. Effect of Varying SiO Contents on Si and FeSi Production. *SSRN Electronic Journal*. [online] https://doi.org/10.2139/ssrn.4118642.

Jusnes, K.F., 2020. *Phase transformations and thermal degradation in industrial quartz*. [online] NTNU. Available at: <https://ntnuopen.ntnu.no/ntnu-xmlui/handle/11250/2675473> [Accessed 30 September 2022].

Kaffash, H., Surup, G.R. and Tangstad, M., 2021. Densification of Biocarbon and Its Effect on CO2 Reactivity. https://doi.org/https://doi.org/10.3390/pr9020193.

Karunanithy, C., Wang, Y., Muthukumarappan, K. and Pugalendhi, S., 2012. Physiochemical Characterization of Briquettes Made from Different Feedstocks. *Biotechnology Research International*, 2012, p.165202. https://doi.org/10.1155/2012/165202.

Lindstad, T., Gaal, S., Hansen, S. and Prytz, S., 2007a. IMPROVED SINTEF SIO-REACTIVITY TEST. INFACON XI. INFACON XI, India. p.10.

Lindstad, T., Gaal, S., Hansen, S. and Prytz, S., 2007b. IMPROVED SINTEF SIO-REACTIVITY TEST. INFACON XI. INFACON XI, India. p.10.

Makgobelele, N.W., Mbaya, R.K.K., Bunt, J.R., Leokaoke, N.T. and Neomagus, H.W.J.P., 2021. Evaluation of the mechanical properties of wood-derived charcoal briquettes for use as a reductant. *Journal of the Southern African Institute of Mining and Metallurgy*, 121(5), pp.187–192. https://doi.org/10.17159/2411-9717/903/2021.

Monsen, B., Tangstad, M., Solheim, I., Syvertsen, M., Ishak, R. and Midtgaard, H., 2007. Charcoal for Manganese Alloy Production. INFACON XI. India. p.14.

Myrhaug, E.H., n.d. Non-fossil reduction materials in the silicon process - properties and behaviour. p.242.

Narron, R., Wolken, G. and Gargulak, J., 2020. Accelerated Polymerization of Ammonium Lignosulfonate from Loblolly Pine. *Forest Products Journal*, 70(1), pp.134–142. https://doi.org/10.13073/FPJ-D-19-00044.

Obi, O.F., Pecenka, R. and Clifford, M.J., 2022. A Review of Biomass Briquette Binders and Quality Parameters. *Energies*, 15(7), p.2426. https://doi.org/10.3390/en15072426.

Olofsson, J., 2025. Multiple Goals for Biomass Residues in Circular Bioeconomies? Assessing Circularities and Carbon Footprints of Residue-Based Products. *Circular Economy and Sustainability*, 5(1), pp.101–123. https://doi.org/10.1007/s43615-024-00428-9.

Olsen, S.E., Tangstad, M. and Lindstad, T., 2026. *Production of Manganese Ferroalloys by Sverre E. Olsen, Merete Tangstad, Tor Lindstad (9788245046144) | Akademika Bokhandel*. [online] Available at: <https://www.akademika.no/realfag/kjemi/production-manganese-ferroalloys/9788245046144> [Accessed 3 July 2026].

Olugbade, T., Ojo, O. and Mohammed, T., 2019. Influence of Binders on Combustion Properties of Biomass Briquettes: A Recent Review. *BioEnergy Research*, 12(2), pp.241–259. https://doi.org/10.1007/s12155-019-09973-w.

Pahnila, M., Koskela, A., Uusitalo, J., Vitikka, O., Sulasalmi, P. and Fabritius, T., 2026. The Effect of Biomass Species and Pyrolysis Method on Biocarbon Briquette Suitability for Submerged Arc Furnace. *Journal of Sustainable Metallurgy*, 12(1), pp.523–536. https://doi.org/10.1007/s40831-025-01343-5.

Prosess21 ekspertgrupperapport, 2021. *Ny prosessteknologi med redusert karbonavtrykk inkl. CCU*. Available at: <https://www.prosess21.no/informasjon-om-prosess21/Download>.

Ringdalen, E., 2014. Quartz properties in the silicon production. *Silicon for the Chemical and Solar Industry XII*.

Schei, A., Tuset, J.K. and Tveit, H., 1998. *Production of high silicon alloys*. [online] Trondheim: Tapir. Available at: <https://urn.nb.no/URN:NBN:no-nb_digibok_2010021004001> [Accessed 12 April 2022].

Smith-Hanssen, N., Jahrsengene, G. and Ringdalen, E., 2023b. Biocarbon Materials in Metallurgical Processes—Investigation of Critical Properties. In: C. Fleuriault, J.D. Steenkamp, D. Gregurek, J.F. White, Q.G. Reynolds, P.J. Mackey and S.A.C. Hockaday, eds. *Advances in Pyrometallurgy*, The Minerals, Metals & Materials Series. Cham: Springer Nature Switzerland. pp.165–177. https://doi.org/10.1007/978-3-031-22634-2_16.

Sommerfeld, M. and Friedrich, B., 2021. Replacing Fossil Carbon in the Production of Ferroalloys with a Focus on Bio-Based Carbon: A Review. *Minerals*, 11(11), p.1286. https://doi.org/10.3390/min11111286.

Tangstad, M. and Ringdalen, E., 2025. Decarbonization Ferroalloy Production Using Biocarbon. *Minerals*, 15(3), p.228. https://doi.org/10.3390/min15030228.

Tuset, J. K and Raaness, O., 1976. *Reactivity of Reduction Materials for the Production of Silicon, Silicon-rich Ferroalloys and Silicon Carbide*.

Zhang, C., Shao, Y., Zhang, L., Zhang, S., Westerhof, R.J.M., Liu, Q., Jia, P., Li, Q., Wang, Y. and Hu, X., 2020. Impacts of temperature on evolution of char structure during pyrolysis of lignin. *Science of The Total Environment*, 699, p.134381. https://doi.org/10.1016/j.scitotenv.2019.134381.

Sethulakshmy Jayakumari
Research Scientist, SINTEF, Trondheim, Norway

I have completed my master's degree in condensed matter physics (2013) and PhD in process metallurgy (2020) from NTNU, Norway. My PhD project focused on silicon carbide formation

during silicon production. I am currently working as research scientist in process metallurgy and raw materials department in SINTEF. I am involved in several research projects related to silicon and manganese production processes. My work focuses on high-temperature furnace experiments, process optimization, raw material characterization, and the development of sustainable metallurgical technologies.
